2003

3-D fracture analysis of circumferentially cracked weld overlay coatings

Erman Citirik
Lehigh University

Citirik, Erman

3-D Fracture Analysis of Circumferentially Cracked Weld Overlay Coatings

May 2003

3-D FRACTURE ANALYSIS OF CIRCUMFERENTIALLY CRACKED WELD OVERLAY COATINGS

by

Erman CITIRIK

A Thesis

Presented to the Graduate and Research Committee

Of Lehigh University

In Candidacy for the Degree of

Master of Science

in

Mechanical Engineering

Lehigh University

MAY 2003

Certificate of Approval

This thesis is accepted and approved in partial fulfillment of the requirements for the Master of Science in Mechanical Engineering.

April 25, 2003
(date)

Thesis Advisor

Chairperson of Department

Acknowledgements

I would like to thank my advisor, Professor Herman F. Nied, for his many suggestions and guidance throughout all of the stages of this research project.

I would also like to acknowledge the support of this research by the participating companies, Pennsylvania Power and Light (PPL), First Energy Corporation and Virginia Power.

Table of Contents

List of tables

List Of Figures

ABSTRACT

Three dimensional fracture analysis of circumferentially cracked boiler tubes is examined using the finite element method. Residual stresses due to welding, temperature values and thermal stresses are computed for five different periodic crack spacing values (h), which are 2, 4, 6, 10 and 20 mm.

ANSYS is used as a preprocessor to generate models for the computation of stress intensity factors due to welding residual stresses. Stress intensity factors are computed with FRAC3D, software developed at Lehigh University. The maximum stress intensity factor is obtained at the deepest penetration of the crack in the model which has the greatest periodic crack spacing, h/2 =10mm. The stress intensity factors due to welding residuals decrease as the crack spacing, h/2 decreases.

Both steady state and transient thermal analyses are performed with ANSYS. These temperature values are input to FRAC3D, to compute stress intensity factors due to thermal stresses. The stress intensity factors due to the steady state conditions are either very small in magnitude or zero, as the crack surface is closed at steady state thermal conditions.

Transient stress intensity factors are also computed. Again, the maximum stress intensity factor is obtained at the deepest point of penetration of the crack in the model for cases with the greatest periodic crack spacing.

1. INTRODUCTION

Transverse cracking in the vicinity of long longitudinal fillet welds is a serious problem in engineering structures. A systematic modeling of a general cracked tubular Y-joint commonly found in offshore structures is described in [1]. Well-graded finite element meshes were generated for a T-joint, which is a specific type of Y-joint, to obtain the stress intensity factors (SIFs) for a surface semi-elliptical crack along the crack tip using quarter-point elements. [1]

Some crack modeling techniques in FE analysis were explained in [2,3]. By mapping circles in two-dimensional planes to three-dimensional intersection curves between tubular members, a complicated three-dimensional mesh generating procedure for tubular joints is changed to a procedure similar to a two-dimensional case. More detailed modeling of welds and cracks can be included to analyze the fracture behavior of cracked tubular joints. Different types of crack tip models are discussed and a four-tip crack model is introduced to model crack propagation. These crack models can be applied to both through-thickness cracks and surface cracks. [2] A new method of fatigue analysis for components is outlined; stress concentrations are analyzed by examining their stress fields and comparing these with the stress fields of cracks of standard geometry. The method was tested by using it to assess three different design conditions for a large cast-iron component. This component suffered fatigue failures from a corner feature, which had a sharp fillet radius. By estimating the stress intensity range, ΔK, in service and comparing this with the threshold value, ΔK_{th}, the in-service observations

could be predicted with a good degree of accuracy. [3] The stress intensity factor is frequently used as a design parameter to quantify the fracture process and it can be used to determine the residual life of a fatigue-damaged structure under conditions of subcritical crack growth.

Transverse cracking in welded structures is strongly influenced by the residual stresses that arise during welding process. Welding is a reliable and efficient metal joining process widely used in industry. Research has been conducted to determine temperature distribution and residual stresses due to welding experimentally in [4,5,6] and computationally in [7,8]. Low carbon steel plates and AISI type 304 stainless steel plates are mostly joined together by multipass welding methods. The temperature distribution that occurs during multipass welding affects the material microstructure, hardness, mechanical properties and the residual stresses that will be present in the welded material. Experimental work was carried out to find out the temperature distribution during multipass welding of the above plates. The temperature distribution curves obtained during the experiments are presented in [4]. The neutron diffraction non-destructive method of measuring residual stresses due to welding is described. Examples of the detrimental residual stress distributions introduced by welding and of the beneficial stresses produced by such processes as autofrettage, cold hole expansion and shot peening are presented. It is demonstrated that, provided an accurate knowledge of the residual stress profiles generated and allowance is made for stress distribution and the multiaxial nature of residual stresses, reliable predictions of fatigue performance can be made. [6]

Residual stress fields are investigated in a welded T-joint, comparing the results computed by three-dimensional models with those computed by two-dimensional models. The study shows that the temperature distribution in the central zone of the joint can be captured successfully by a two-dimensional finite element model and a technique that takes into account the heat transfer balance and welding speed. The residual stresses in the plane of the two-dimensional model computed by this method show fairly good agreement with those computed by the three-dimensional model. [7]

Welding is a process for joining similar metals. Welding joins metals by melting and fusing; the base metals being joined and the filler metal applied. Welding employs pinpointed, localized heat input. Most welding involves ferrous-based metals such as steel and stainless steel. Welding covers a temperature range of 1500° F - 3000° F (800°C - 1635°C). Weld joints are usually stronger or as strong as the base metals being joined. Typically, welding is used for forging, blacksmithing, oil pipelines, and food equipment applications. Weld overlay is used to strengthen the fireside of the boiler tube against corrosion and erosion. GMAW is one of the most commonly used welding processes in boiler tubes to weld the overlay.

1.1 Welding Parameters in GMAW

In GMAW, metals are melted and joined by heating them with an arc established between a continuously fed filler wire electrode and the metals as shown in Figure 1.1. Shielding of the arc and the molten weld pool is often obtained by using inert gases such as argon and helium, and this is why GMAW is also called the metal-inert gas (MIG)

welding process. Since noninert gases, particularly CO_2, are also used, GMAW seems a more appropriate name. Like gas-tungsten arc welding (GTAW), GMAW can be very clean when using an inert shielding gas. The main advantage of GMAW over GTAW is the much higher deposition rate, which allows thicker workpieces to be welded at higher welding speeds. GTAW requires more skill than GMAW. However, GMAW guns can be bulky and difficult to reach small areas or corners. [9]

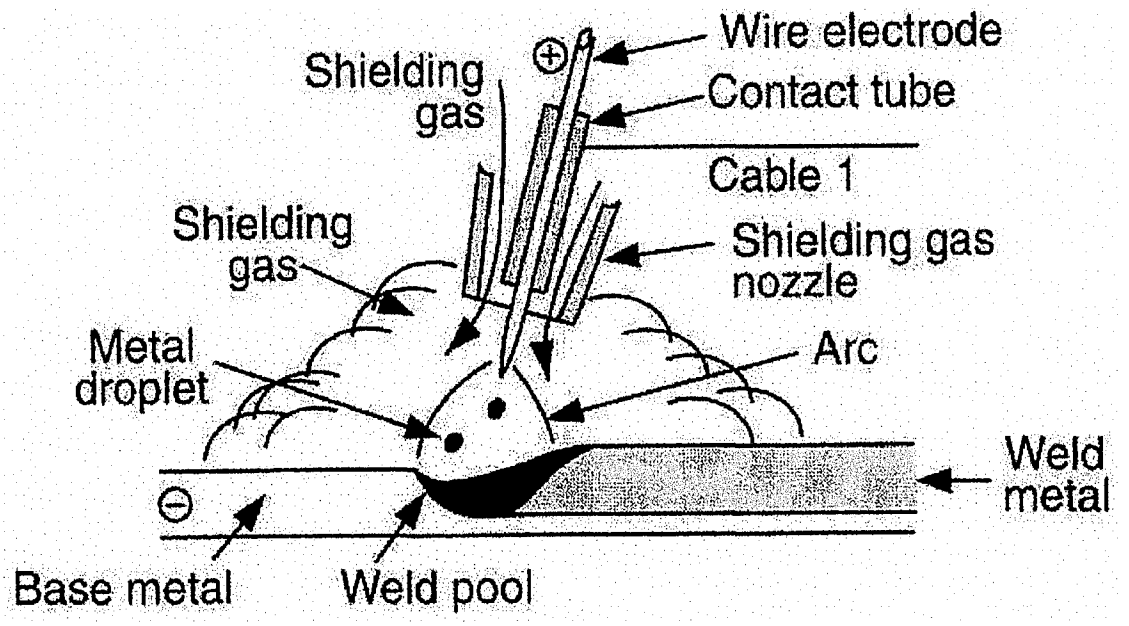

Figure 1.1: GMAW (welding area enlarged) [9]

In arc welding processes a number of welding parameters exist that can affect the size, shape, quality and consistency of the weld. The major parameters that affect the weld include weld current, arc voltage, and travel speed. The sizes and types of electrodes for shielded metal arc welding define the arc voltage requirements and the amperage requirements. The current may be either alternating or direct, but the power source must be able to control the current level in order to respond to the complex

variables of the welding process itself. As direct current electrodes perform well at low amperage, they are often selected for welding thin metals. Most covered electrodes operate best with electrode positive (reverse polarity), which produces the deepest penetration. Electrode negative operation might produce a higher melting rate. The secondary variables include the angle of the electrode to the work, the angle of the work itself, the thickness of the flux layer, and the arc length. How to determine the correct amperage for a certain electrode will depend on the size and classification of the electrode. Even the type of joint and welding position must be considered. The process requires sufficient electric current to melt both the electrode and a proper amount of base metal. The penetration goes deeper as the current increases. Using too high amperage may cause problems such as excessive spatter, electrode overheating and cracking. The arc voltage is varied within narrower limits than welding current. It has an influence on the bead width and shape. Higher voltages will cause the bead to be wider and flatter. Extremely high arc voltage should be avoided, since it can cause cracking. Low arc voltage produces a stiffer arc that improves penetration. If the voltage is too low, a very narrow bead will result. The speed the electrode travels along the joint has a direct influence on bead shape, depth of fusion, cosmetic appearance and heat input into the base metal. Faster travel speeds produce narrower beads that have less penetration. This can be an advantage for sheet metal welding where small beads and minimum penetration are required. Travel speed also affects heat input, which in turn influences the metallurgical structure of the weld metal. The cooling rate increases or decreases proportionately with the travel speed. Also, the heat-affected zone, where the peak temperatures are too low to cause melting but high enough to cause the microstructure

and the properties of the materials to change significantly, will increase in size and the cooling rate decreases. If speeds are too fast, however, there is a tendency for undercut and porosity, since the weld freezes quicker. Arc length refers to the distance from the molten tip of the electrode core to the molten weld pool. Generally, arc length increases as the size of the electrode and amperage increase. Limiting arc length to the diameter of the core rod of the electrode is a good guideline. [14]

1.2 Residual Stresses During GMAW

Residual stresses are stresses that would exist in a body if all external loads were removed. They are sometimes called internal stresses. Residual stresses that exist in a body that has previously been subjected to nonuniform temperature changes, such as those during welding, are often called thermally induced residual stresses. FEM codes (HEAT2D AND FRAC2D_WELD) [11] developed at Lehigh University were used to perform thermal and mechanical analyses. The problem was treated as an uncoupled thermal and mechanical problem; first the temperature distribution due to welding was determined by using HEAT2D, and residual stresses were determined by FRAC2D_WELD using HEAT2D results.

1.3 Transient Stresses

Thermal fatigue is one of the causes of crack initiation and the propagation of circumferential cracks in boiler tubes. Thermal stresses are caused by temperature

gradients and differences in thermal expansion coefficients. Steady state thermal stresses are similar to residual stresses, remaining constant in time. They do not have any effect on fatigue life, which is controlled by changes in the stress state. However, steady state and residual stresses determine the initial crack length. The main difference in the steady state and transient analyses is that an applied load in transient analysis is a function of time. Time dependent loads such as transient stresses and other dynamic loads are the main reasons for fatigue crack growth. Transient thermal stresses are caused by soot blowing operations in boiler tubes, which are performed to have a higher thermal efficiency.

1.4 Fracture Mechanics – Stress intensity Factors

The mode I stress intensity factor, K_I, is commonly used in fracture mechanics to accurately predict the stress state ("stress intensity") near the tip of a crack caused by a remote load or residual stresses. When this stress state becomes critical a small crack grows ("extends") and the material fails. The stress intensity factor is dependent on the body geometry, crack size, load level and load configuration. For some common geometries and specimens, the analytical expressions to determine SIFs are available in many handbooks and other references. However, there is no analytical solution of the complex geometries examined in this study. Therefore FEM was used to determine SIFs computationally.

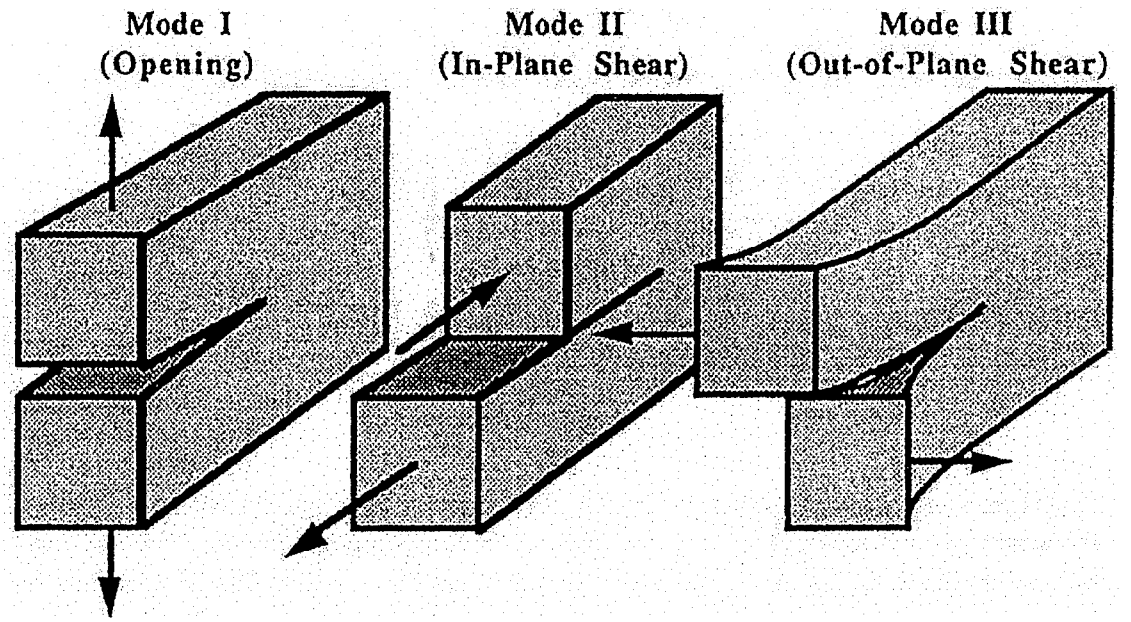

Figure 1.2: Basic modes of loading

Generally there are three modes to describe different crack surface displacement as shown in Figure1.2. In this study we are only concerned with mode I (K_I) cracking behavior. Mode I is the opening or tensile mode, where the crack surfaces move directly apart. Mode II is sliding or in-plane shear mode where the crack surfaces slide over one another. Mode III is tearing and anti-plane shear mode where the crack surfaces move out of plane relative to one another. In this study, SIFs are determined by using enriched 3-d crack tip elements. [13]

Boiler tubes are commonly used in chemical plants, refineries and power generation plants. These tubes often operate under extreme temperatures and pressures that can cause them to fail. Boiler tubes can become weakened by fireside erosion and corrosion. As mentioned previously, weld overlay can be applied to solve this problem.

The boiler tube materials are generally SA213/T22, T11 or T12 type steel. The overlay coating material is usually a high temperature alloy such as S309 steel, Inconel625 or Inconel622. Weld overlay coatings provide improved resistance to erosion and corrosion, without adversely affecting the boiler's heat transfer characteristics. Overlays can significantly increase boiler tube life. Weld overlay is used to protect the fireside surface, while also adding additional material to this same surface. Weld overlay coatings are susceptible to circumferential cracking in low NOx combustion environments in power plants. [15] A picture of a cracked boiler tube panel section is shown in Figure 1.3. 'h' is the periodic crack spacing in the boiler tube.

Fracture analysis of the boiler tubes considered in this study is divided into three parts. The first part is determination of SIFs due to residual stresses caused by welding. The second part is determination of SIFs due to steady state thermal stresses. The third part is determination of SIFs due transient thermal stresses. The first two parts play a role in determination of the initial crack length, they do not have any effect on the fatigue life of boiler tubes. The transient thermal stress is the main concern for fatigue life assessment.

The soot blowing operation seems to be the main cause to have transient thermal stresses. Soot blowing is performed to periodically remove accumulated slag and ash deposits from the tube surfaces. This procedure significantly improves the heat transfer between the fireside and the steam inside the boiler. Coal-fired units require large numbers of permanently installed soot blowing equipment. Superheated steam or compressed air is the medium used to remove deposits, employing a short, single-nozzle retractable blower and cleaning a surface with a five-foot radius. The approximate

duration of soot blowing operation lasts for approximately two minutes with a 100 °C steam temperature. These values vary according to the power plant type and slag thickness. In this study, it is assumed that the temperature of the fireside surface, which is 400 °C at steady state, decreases to a lower value than 400 °C in order to obtain tensile stresses. The two cases, which are examined including ΔT=50 °C and ΔT=75 °C, are considered as reference temperature changes in the problem. All calculations in this study are performed considering five different periodic crack spacings: h/2=10mm, h/2=5mm, h/2=3mm, h/2=2mm and h/2=1mm.

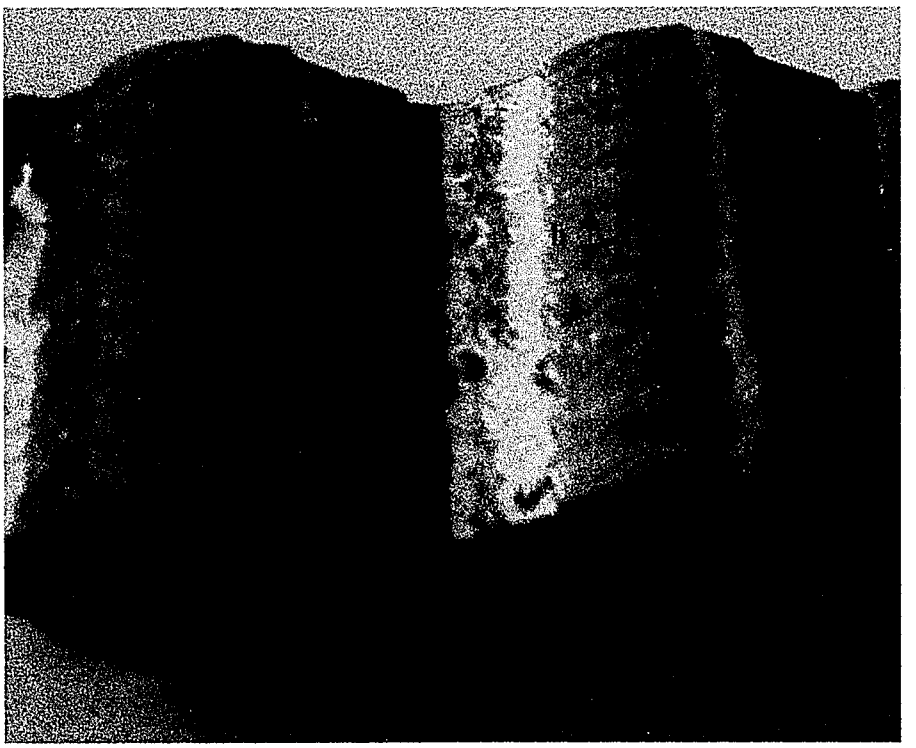

Figure 1.3: Picture of the boiler tube panel section, h = periodic crack spacing

duration of soot blowing operation lasts for approximately two minutes with a 100 °C steam temperature. These values vary according to the power plant type and slag thickness. In this study, it is assumed that the temperature of the fireside surface, which is 400 °C at steady state, decreases to a lower value than 400 °C in order to obtain tensile stresses. The two cases, which are examined including ΔT=50 °C and ΔT=75 °C, are considered as reference temperature changes in the problem. All calculations in this study are performed considering five different periodic crack spacings: h/2=10mm, h/2=5mm, h/2=3mm, h/2=2mm and h/2=1mm.

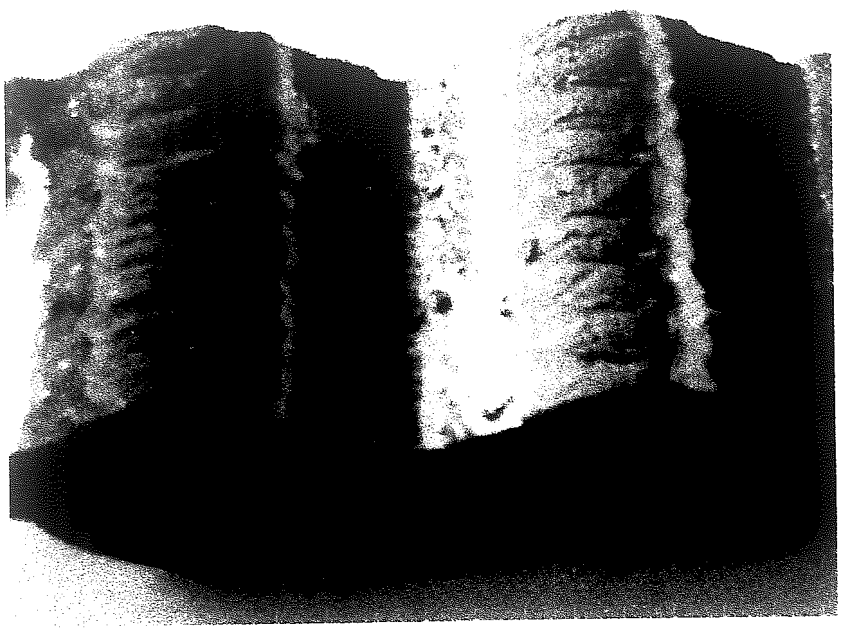

Figure 1.3: Picture of the boiler tube panel section, h = periodic crack spacing

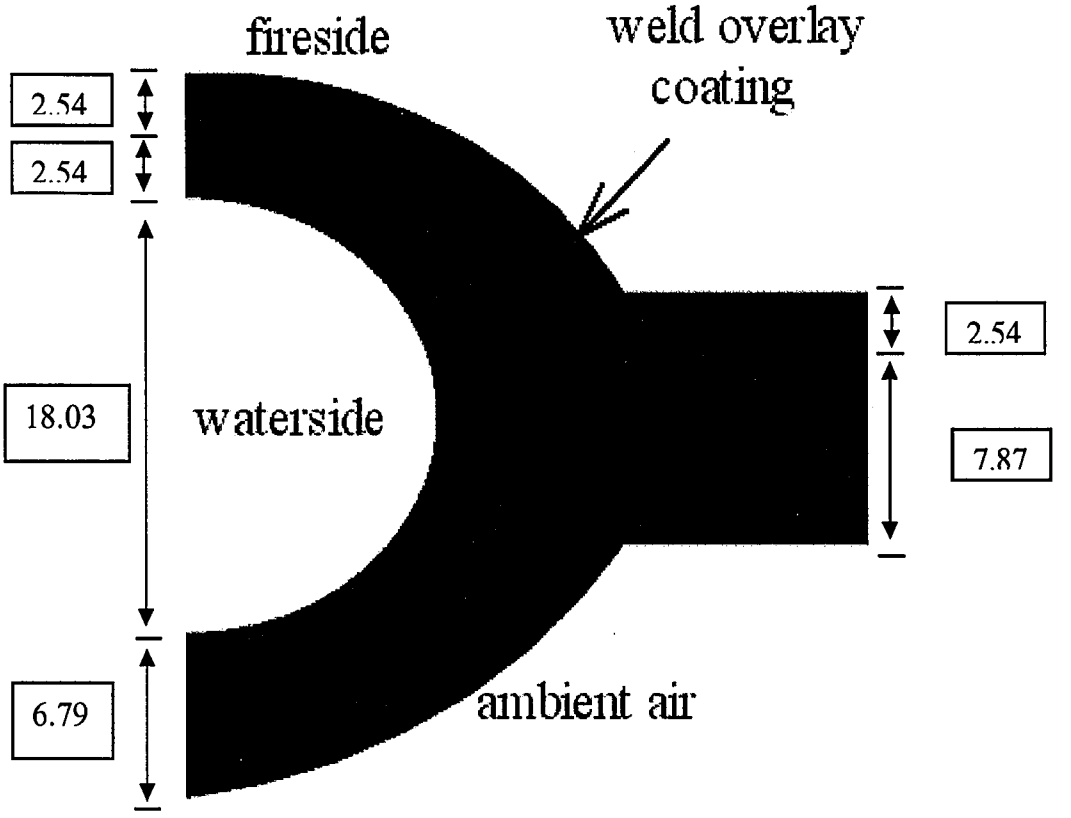

Figure 1.4: Dimensions of the boiler tube used in the half model (mm)

The measured dimensions of the boiler tube are shown in Figure 1.4. Half of the boiler tube is modeled considering symmetric boundary conditions. Even though the waterside area in this figure is circular, the outside of the boiler is non-circular.

2. Thermal Analysis

The steady state and the transient thermal analyses are performed using ANSYS. The basis for thermal analysis in ANSYS is a heat balance equation obtained from the principle of conservation of energy. The finite element solution performed with ANSYS calculates nodal temperatures, and then uses the nodal temperatures to calculate other thermal quantities. [10]

A steady-state thermal analysis calculates the effects of steady thermal loads on a system or a component. Half of the boiler geometry was modeled in 3-d considering the symmetric boundary conditions for the steady state and the transient analyses. The 3-d element used for both steady and transient analyses is a 20-node thermal solid element (PLANE90), which has one degree of freedom, temperature at each node. Three dimensional finite element model is shown in Figure 2.1.

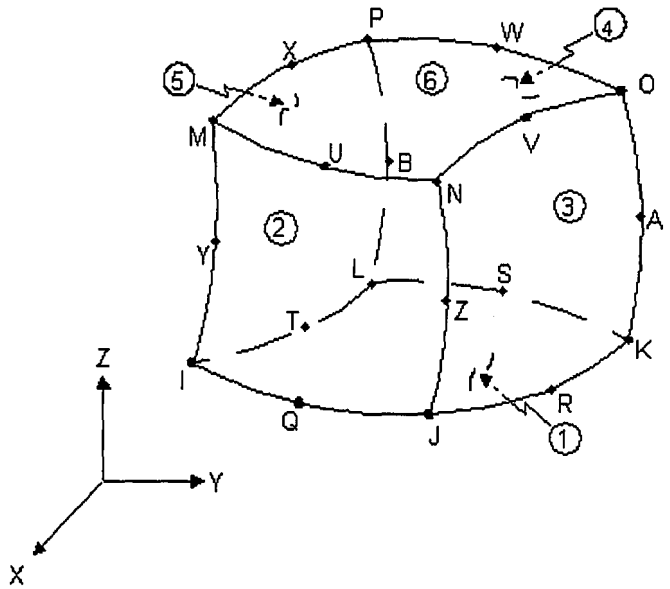

Figure 2.1: 3-d solid finite element model for thermal analysis [10]

Temperature values at each node are used as boundary conditions to determine stress intensity factors for steady state case. The boundary conditions for steady state are used from [12] and shown in Table 2.1.

Boundary	Temperature (°C)
Waterside	370
Fireside	400
Ambient-side	Convection (h=5 $W/m^2.C$, T_0=200 °C)

Table 2.1: Thermal boundary conditions for steady state

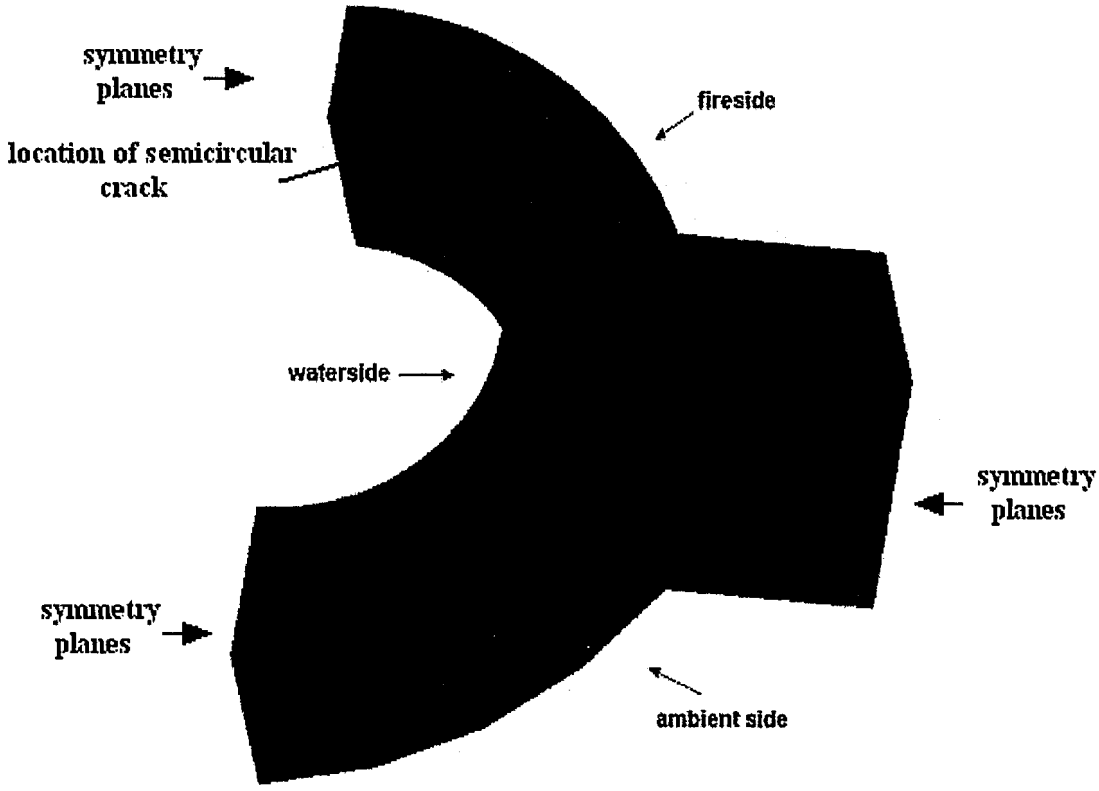

Figure 2.2: 3-d finite element model of a boiler tube

Temperature values at each node are used as boundary conditions to determine stress intensity factors for steady state case. The boundary conditions for steady state are used from [12] and shown in Table 2.1.

Boundary	Temperature (°C)
Waterside	370
Fireside	400
Ambient-side	Convection (h=5 $W/m^2.C$, T_0=200 °C)

Table 2.1: Thermal boundary conditions for steady state

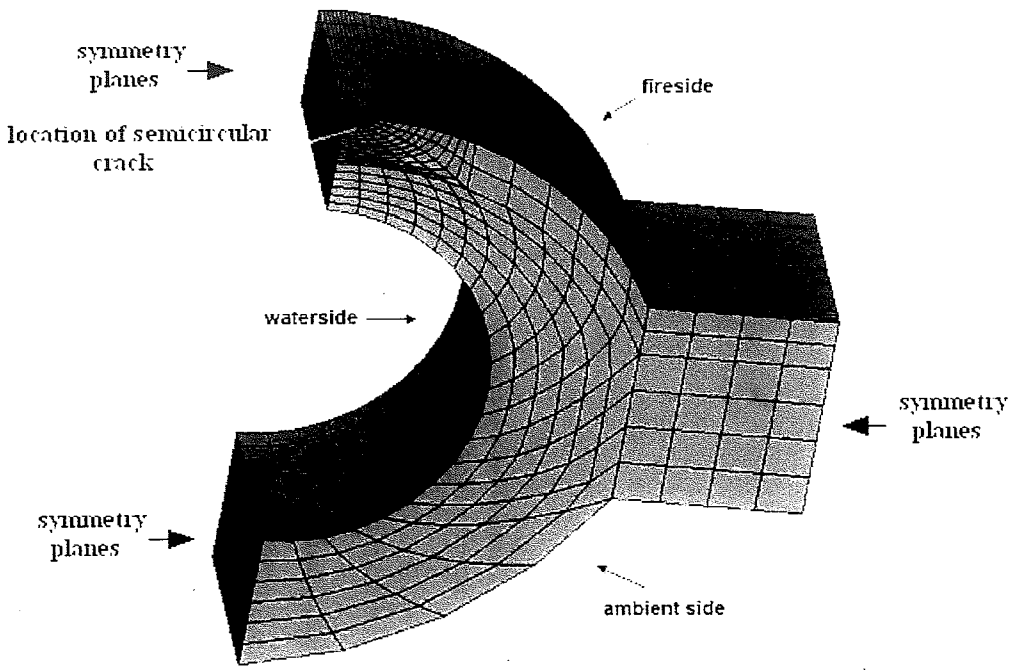

Figure 2.2: 3-d finite element model of a boiler tube

	SA213/A		309S	
T (°C)	k (w/m^2)	k/ρc (m^2/sec)	k (w/m^2)	k/ρc (m^2/sec)
21.1	42.9	12.44E-6	9	3.25E-6
500	34.1	6.880E-6	13.8	4.20E-6
1200	22.3	5.800E-6	19.3	5.40E-6
	For all temperatures;			
	ρ=7900 (kg/m^3)		ρ=7950 (kg/m^3)	
	k: thermal conductivity, ρ: density, c: specific heat			

Table 2.2: Thermal properties of the pipe and the coating material as a function of temperature [11]

The thermal material properties in Table 2.2 are used in all thermal calculations. The steady state temperature distributions for five different h/2 values are computed and all of them have the same temperature distribution. The temperature distribution is independent from the periodic crack spacing. Temperature distribution of "h/2=10mm model" at steady state is shown in Figure 2.3.

The biggest three-dimensional finite element model, which has 14457 nodes and 3000 elements used in some computations is shown in Figure 2.2. The smallest three-dimensional finite element model used in some computations has 5035 nodes and 900 elements.

Both axisymmetric and 3-d model are used in transient thermal calculations considering the symmetric boundary conditions within the model. Of course, the 3-d model is more realistic but the axisymmetric model is very useful for obtaining a preliminary knowledge about the stress behavior around the crack region. An axisymmetric structure (defined with the axial direction along the global Y axis and the radial direction parallel to the global X axis) is represented by a plane (X, Y) finite element model. The dimensions of the axisymmetric model used are shown in Figure 2.3. The main advantage of using the axisymmetric model is that the analysis time is much shorter compared to that of an equivalent three-dimensional model. The results from axisymmetric and 3-d models are consistent to each other. The temperature distribution of 3-d model is shown in Figure 2.4 and the temperature distribution of the axisymmetric model is shown in Figure 2.5 for the steady state conditions. All graphs are from the axisymmetric model and all contour plots are from the 3-d model.

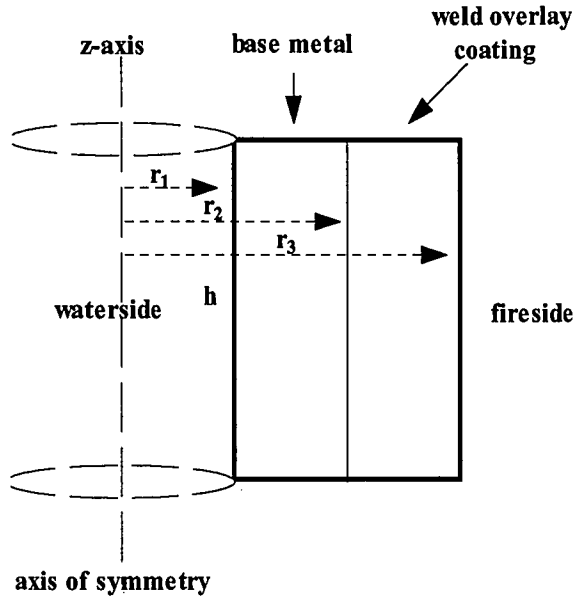

Figure 2.3: Axisymmetric model of the boiler tube to obtain preliminary knowledge about the stress behavior around the crack region (r_1=3mm, r_2=6.2mm, r_3=9.2mm, h=10mm)

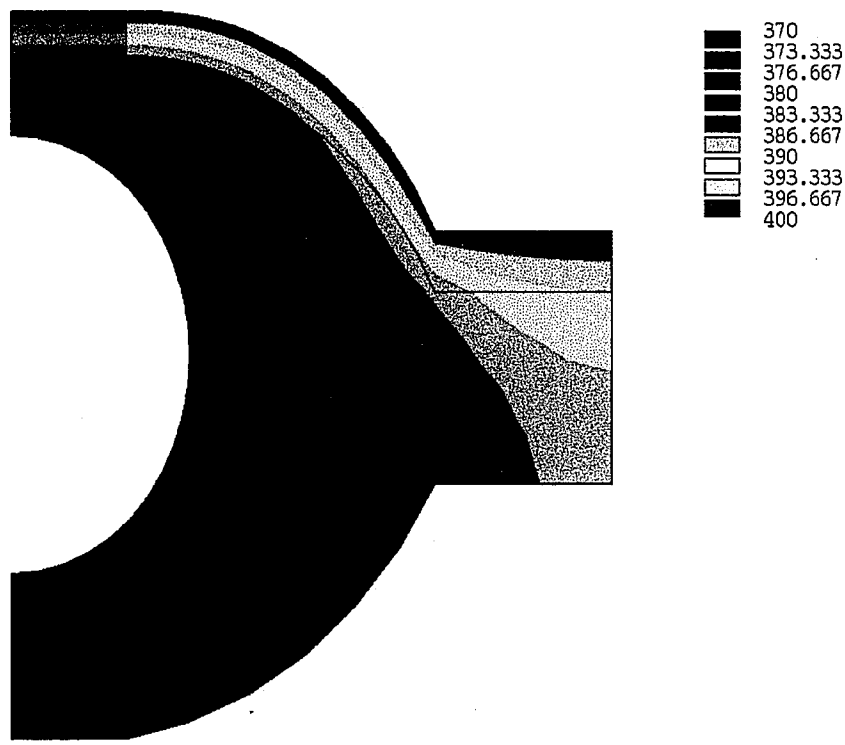

Figure 2.4: Temperature distribution of "h/2=10mm model" at steady-state

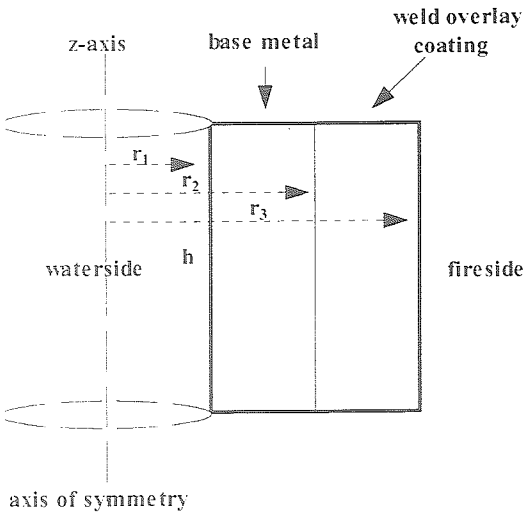

Figure 2.3: Axisymmetric model of the boiler tube to obtain preliminary knowledge about the stress behavior around the crack region (r_1=3mm, r_2=6.2mm, r_3=9.2mm, h=10mm)

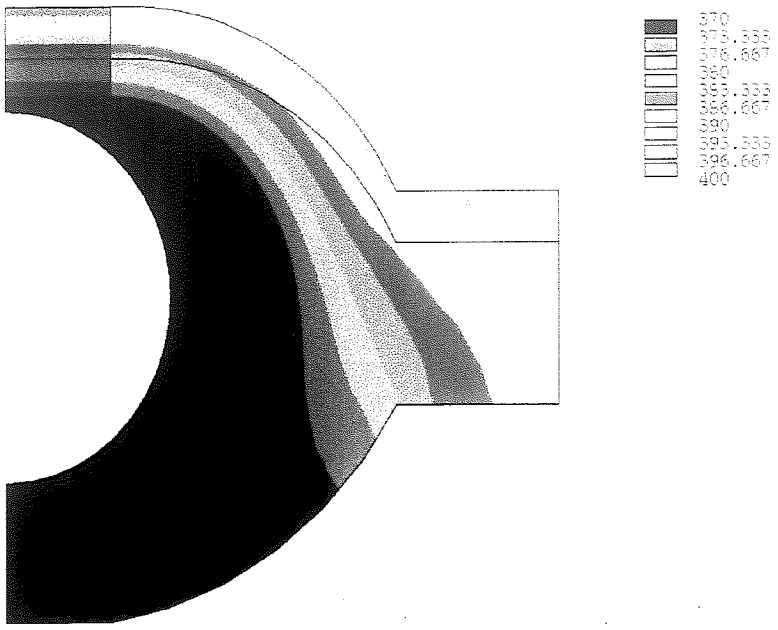

Figure 2.4: Temperature distribution of "h/2=10mm model" at steady-state

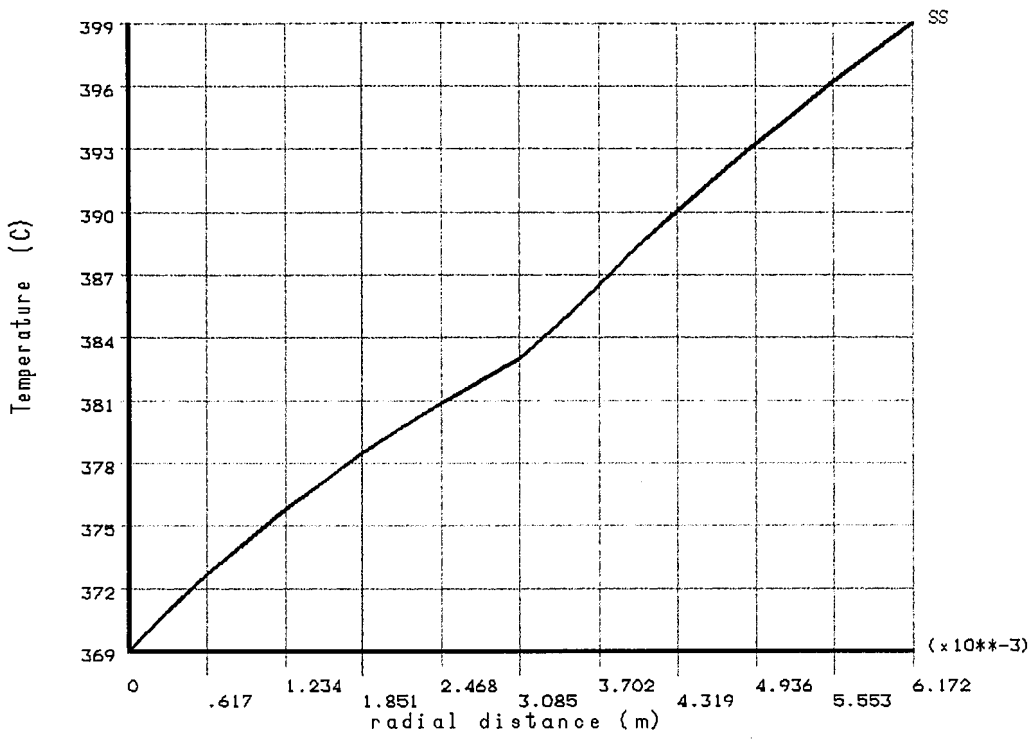

Figure 2.5: Temperature distribution in the axisymmetric model at steady state

The temperature boundary conditions are shown as a function of time in Figure 2.6 which is for ΔT=50 °C on the outer surface and in Figure 2.8 for ΔT=75 °C. The corresponding transient temperature distributions are shown in Figures 2.7 and 2.9, respectively. The transient analyses were performed by using parametric language of ANSYS. The input file used to perform transient thermal and mechanical computations is in the Appendix.

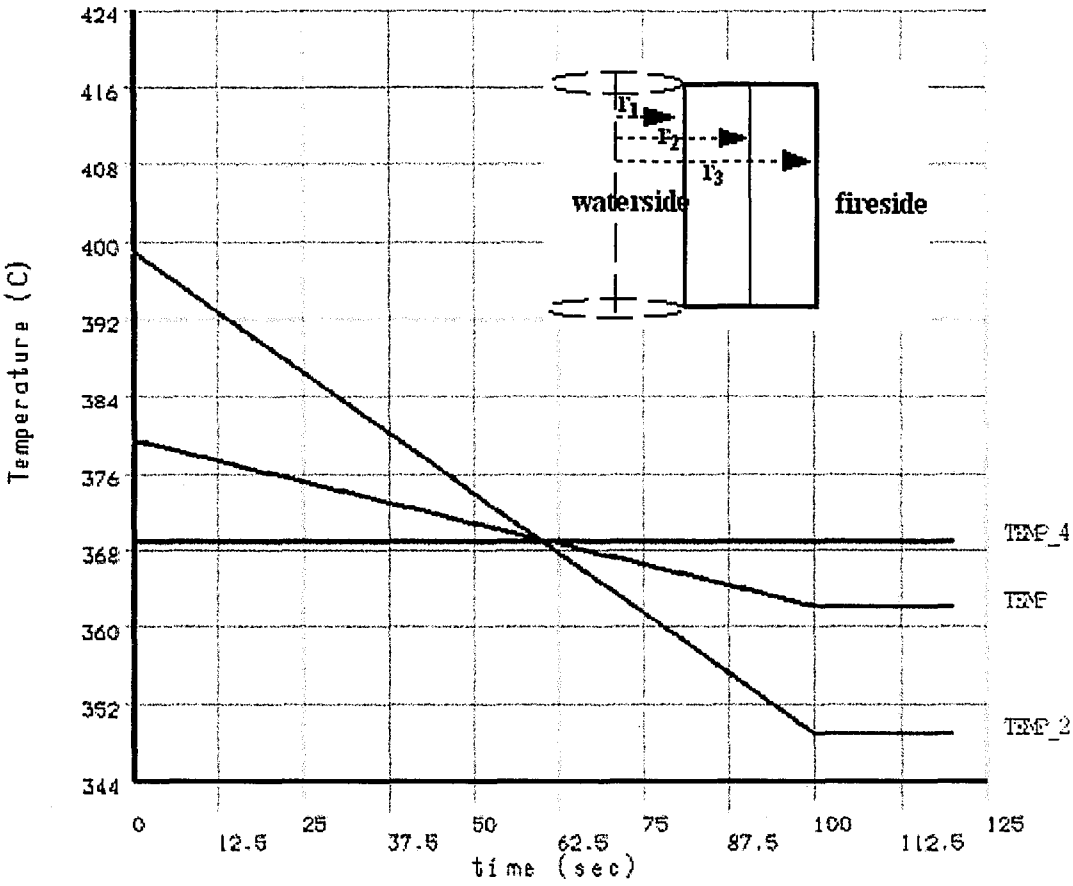

TEMP_2: A point from the fireside at $r=r_3$

TEMP: A point between the fireside and the waterside at $r=r_2$

TEMP_4: A point from the waterside at $r=r_1$

Figure 2.6: Temperature boundary conditions for $\Delta T=50$ °C on outer surface

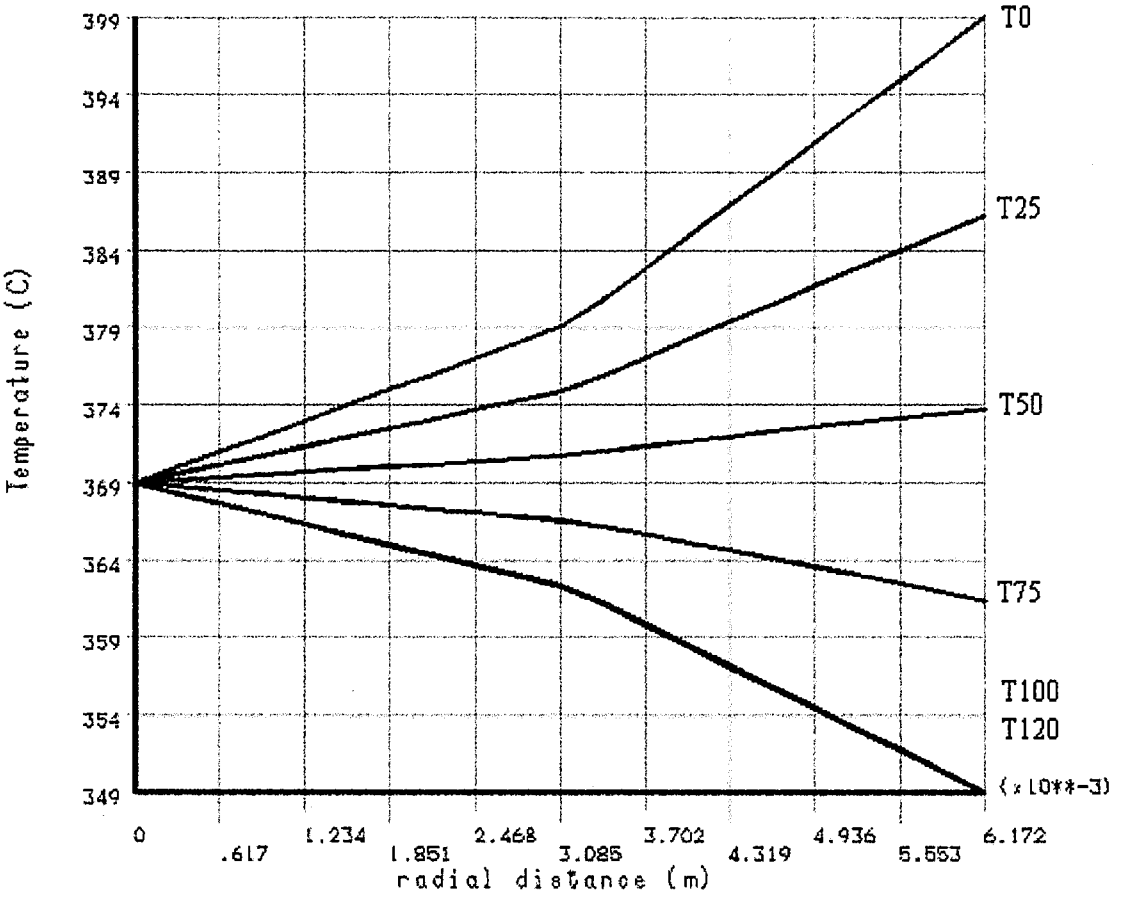

T0 :Temperature at time 0 sec

T25 :Temperature at time 25 sec

T50 :Temperature at time 50 sec

T75 :Temperature at time 75 sec

T100:Temperature at time 100 sec

T120:Temperature at time 120 sec

Figure 2.7: Temperature distribution through the boiler tube wall in the transient analysis for ΔT=50 °C on outer surface

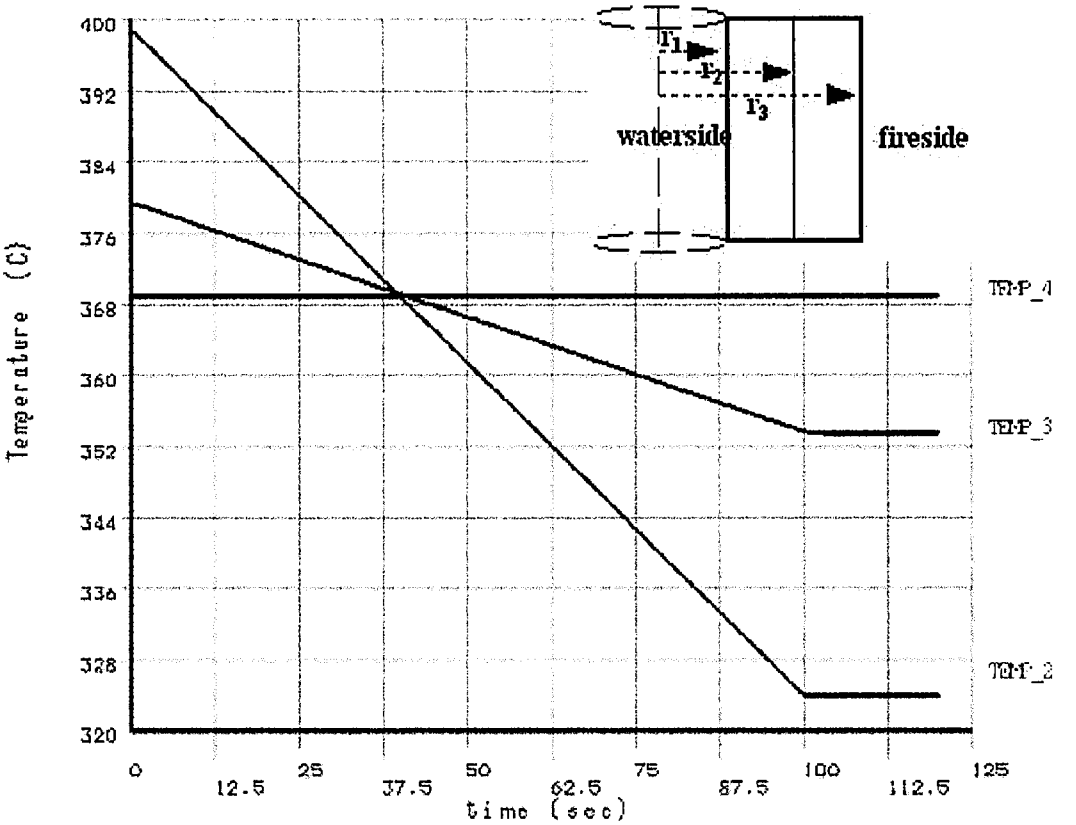

TEMP_2 : A point from the fireside at $r=r_3$

TEMP_3 : A point between the fireside and the waterside at $r=r_2$

TEMP_4 : A point from the waterside at $r=r_1$

Figure 2.8: Temperature boundary conditions for $\Delta T=75$ °C on outer surface

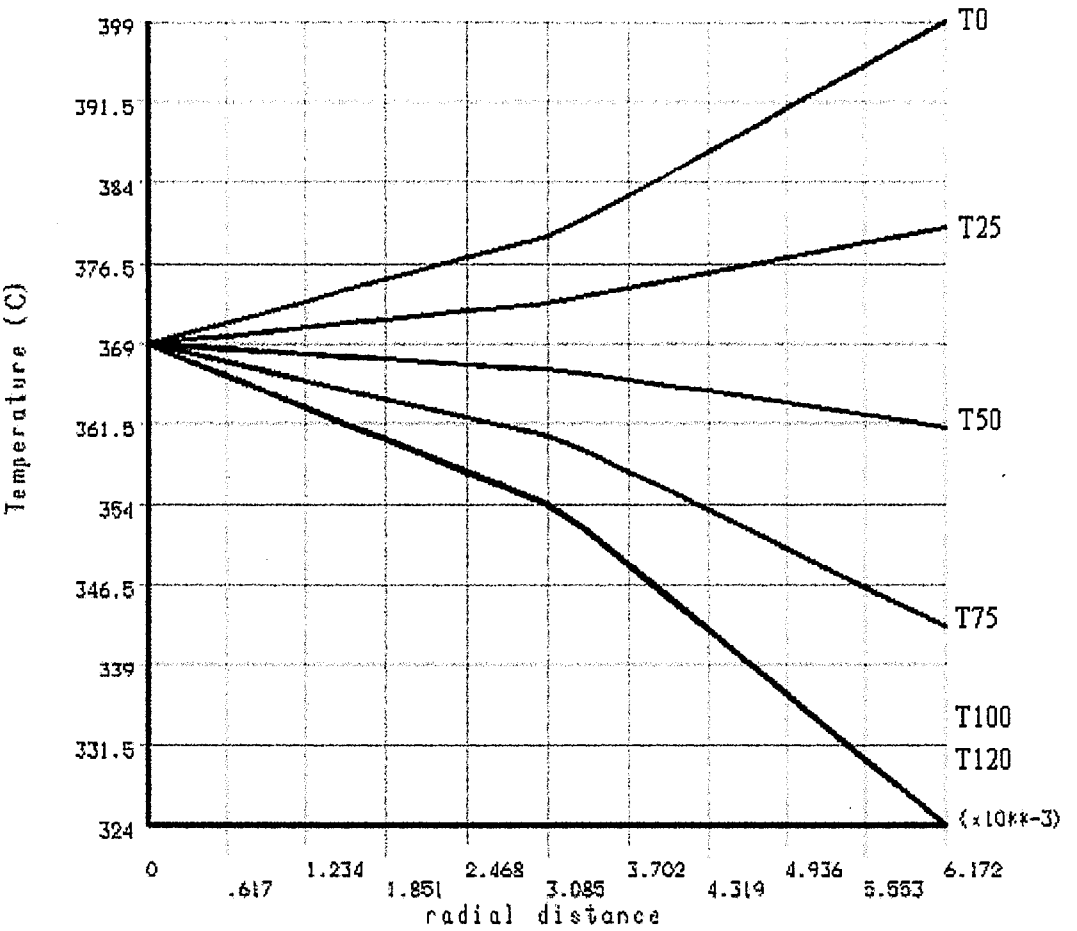

T0 : Temperature at time 0 sec

T25 : Temperature at time 25 sec

T50 : Temperature at time 50 sec

T75 : Temperature at time 75 sec

T100: Temperature at time 100 sec

T120: Temperature at time 120 sec

Figure 2.9: Temperature distribution through the boiler tube wall in the transient analysis for ΔT=75 °C on outer surface

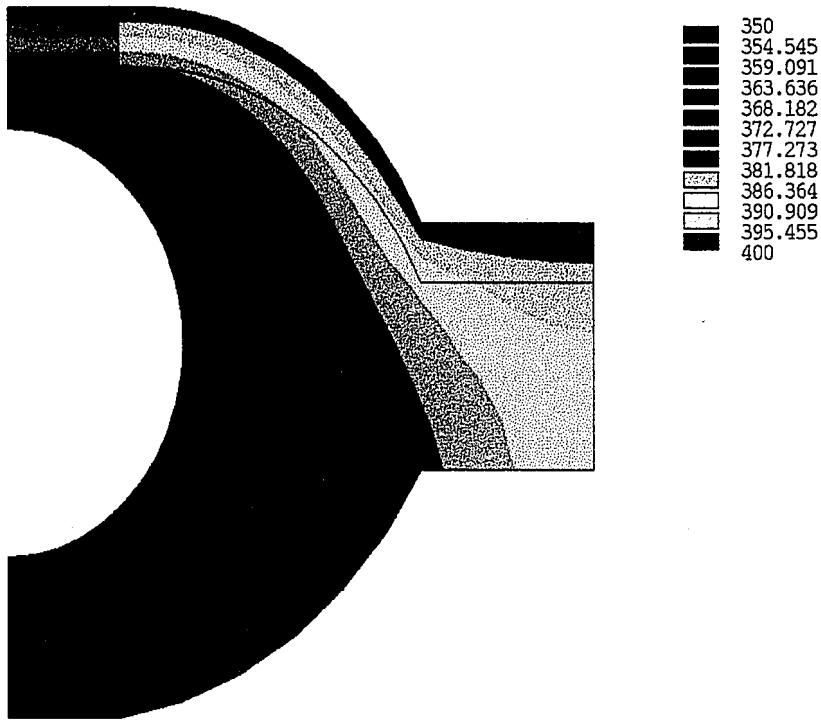

Figure 2.10: Temperature distribution in the transient analysis for ΔT=50 °C at t=0 sec

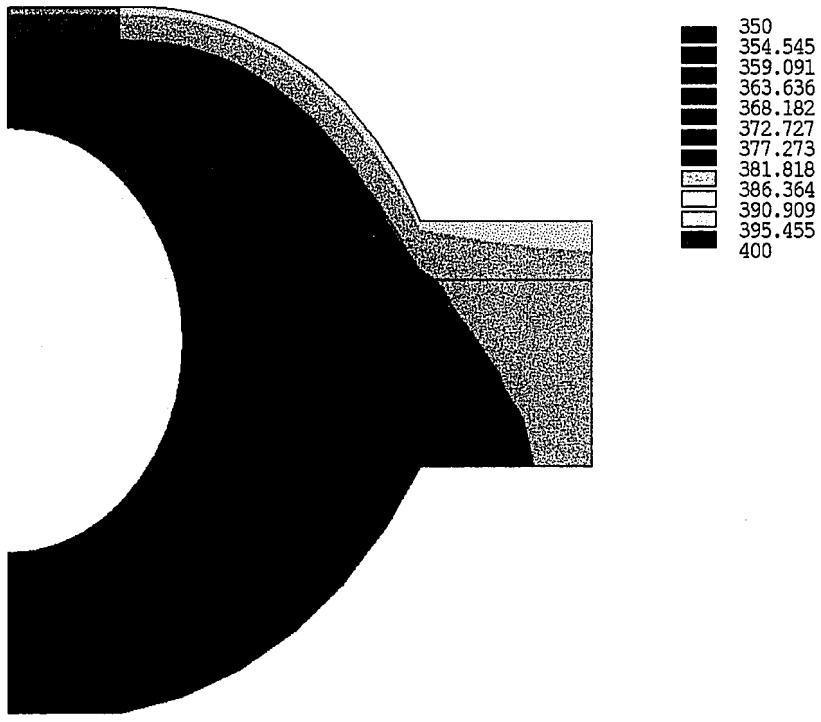

Figure 2.11: Temperature distribution in the transient analysis for ΔT=50 °C at t=24 sec

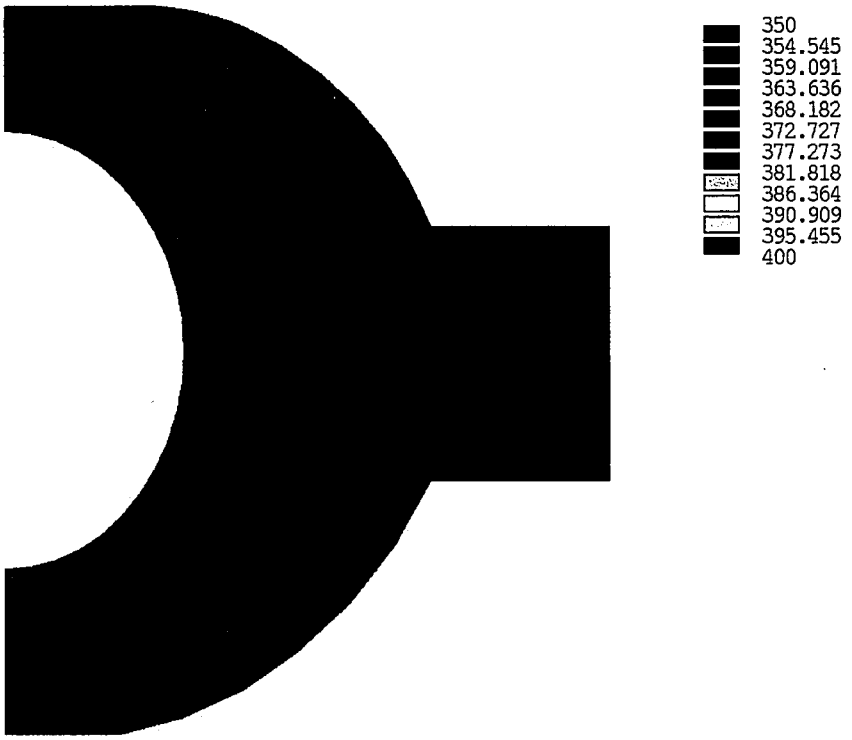

Figure 2.12: Temperature distribution in the transient analysis for ΔT=50 °C at t=36 sec

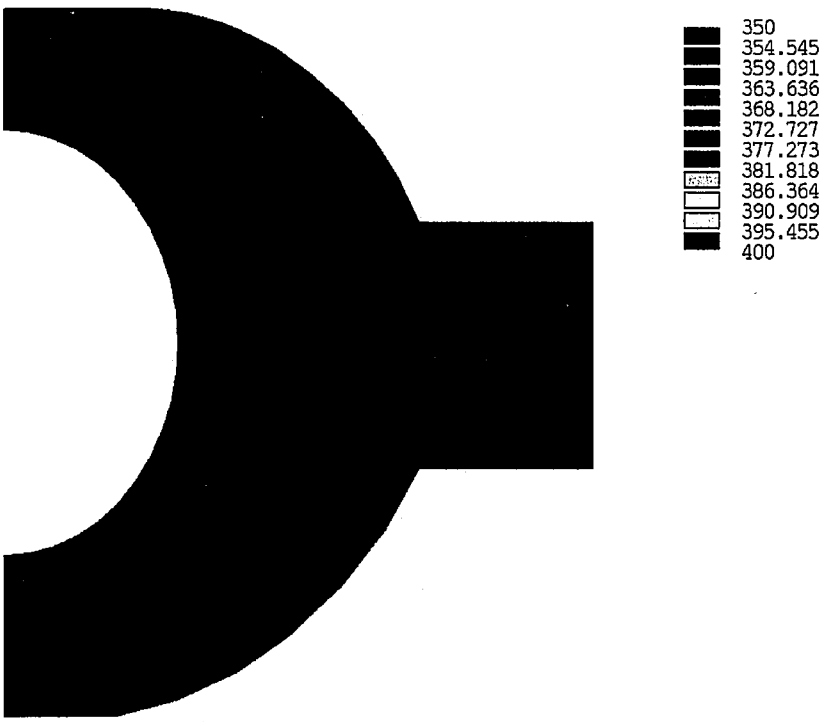

Figure 2.13: Temperature distribution in the transient analysis for ΔT=50 °C at t=52 sec

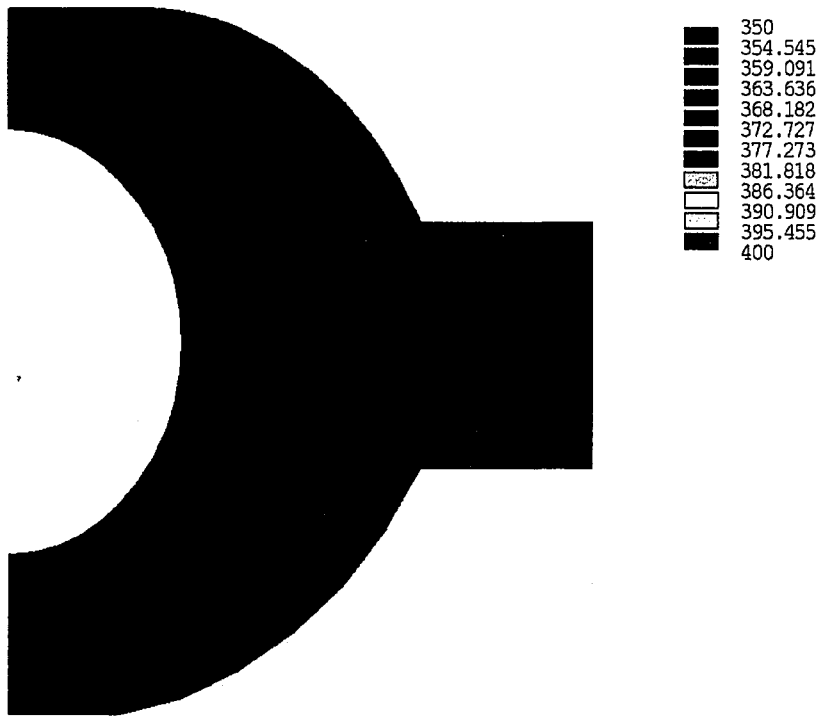

Figure 2.14: Temperature distribution in the transient analysis for ΔT=50 °C at t= 76 sec

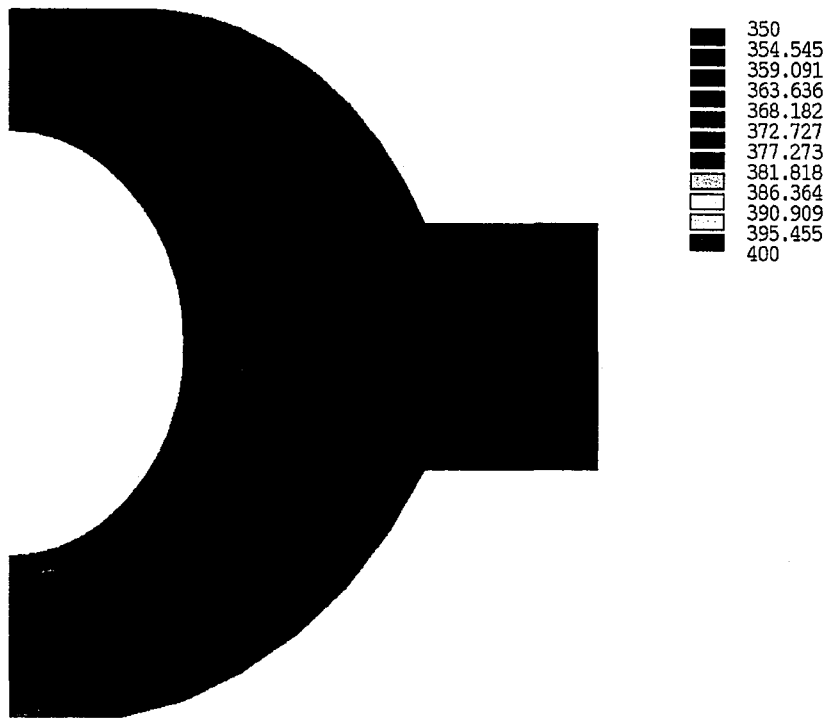

Figure 2.15: Temperature distribution in the transient analysis for ΔT=50 °C at t= 100 sec

3. Structural Analysis

Three different stresses are considered to get the stress state that is thought to result in surface cracking. These are residual stresses due to welding, steady state thermal stresses due to temperature difference between the waterside and the fireside and the transient thermal stresses caused by soot blowing operations.

Residual stresses in weld overlay operations have been shown to be equal to the yield strength of the material. [11] These residual stresses were calculated by using Heat2d and Frac2d_weld programs developed at Lehigh University.

Thermal stress is introduced within a body with changes in temperature. The region of material which has a higher temperature generally produces a larger thermal expansion than regions with lower temperatures. Hence, for the boiler tube, the warmer side of the tube is in compression and the cool boundary is in tension. In a soot blowing operation, the temperature of the fireside decreases to a lower value. The larger the temperature drop or temperature gradient, the more severe the thermal stresses.

In order to compute the stresses in the tube after the thermal analysis, the thermal element should be replaced by an equivalent structural element. Thermal stress solutions are thus obtained from two ANSYS analyses in sequence;

1. The first analysis solves for the temperature distribution within the model from the given thermal boundary conditions.
2. Then the nodal temperatures from the thermal analysis are directly input to an ANSYS structural analysis.

The material properties given in Table 3.1 were used in the stress analyses.

	SA213/A		309S	
T (°C)	E (GPa)	α (1/°C)	E (GPa)	α (1/°C)
21.1	205	1.10E-5	210	1.55E-5
500	170	1.50E-5	120	1.78E-5
1200	110	1.87E-5	103	2.0E-5
	Sy=200 Mpa, v=0.3		Sy=160 Mpa, v=0.27	

E: young's modulus, α: coefficient of thermal expansion, v: poisson's ratio

Table 3.1: Mechanical Properties of the pipe and clad material as a function of Temperature [11]

Boundary conditions are applied as given in Table 3.2 where u, v and w are the x, y and z components of the displacement, h is the surface crack spacing, 'a' is the width of the model in x direction, 'b' is the thickness of the model in y direction. The most realistic and appropriate boundary condition at the z= h/2 plane, is tied-nodes, which simulates periodic boundary conditions, but when tied-nodes are defined as a boundary it causes a significant increase in computation time. Therefore, fixed boundary conditions were used on the z=h/2 in most cases. It is shown in Chapter 4, that whether fixed or tied nodes are specified, the SIFs determined from these calculations are almost the identical. The mechanical boundary conditions are shown in Figures 3.1 and 3.2. Since we are primarily interested in the stresses around the crack region, internal steam pressure is ignored.

Plane	Boundary
z=0	w=0
z=h/2	w=0
x=0	u=0
x=a	u=0
x=a, y=b/2	v=0

Table 3.2: Mechanical boundary conditions for stress analysis

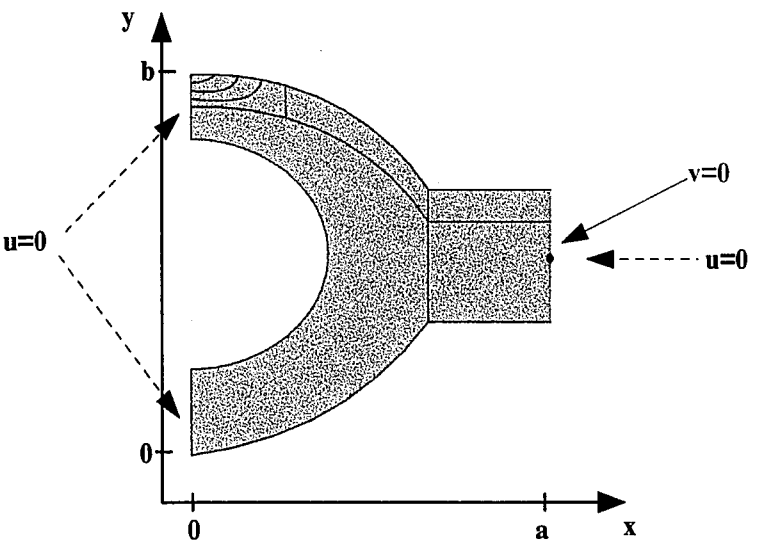

Figure 3.1: Mechanical boundary conditions in the x-y plane, front view of the model

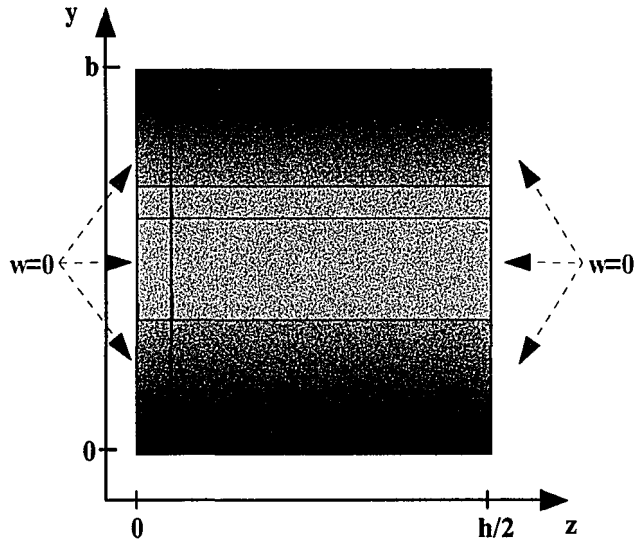

Figure 3.2: Mechanical boundary conditions in the z-y plane, right view of the model

The same three-dimensional finite element model used in thermal calculations, which has 14457 nodes and 3000 elements, was used in some computations to obtain transient thermal stresses. Automatic time stepping was used in the analyses and it took around four hours to ANSYS to complete transient thermal stress analysis.

Figures 3.3 and 3.4 depict the steady state axial stresses in the boiler tube. Since the fireside is warmer than the waterside at steady state, there is compression at the fireside and tension at the waterside. This compression will result in negative stress intensity factors for cracks on the outer surface.

Transient stresses are shown in Figures 3.5 to 3.12. The temperature of the fireside starts to decrease due to a simulated soot blowing operation. The compression at the fireside changes to tension as the temperature drops.

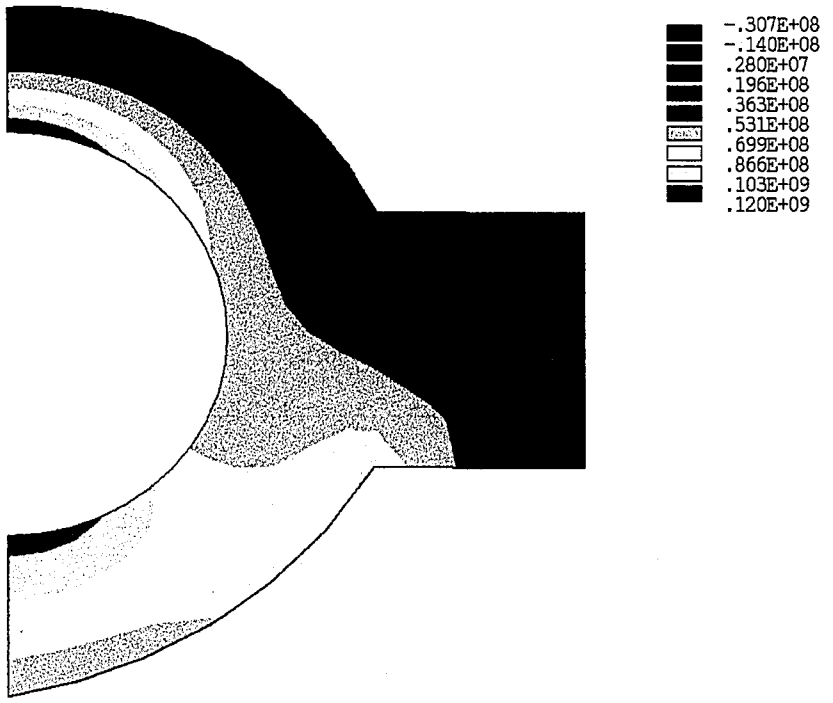

Figure 3.3: Steady state thermal stress from the front view, σ_{zz}

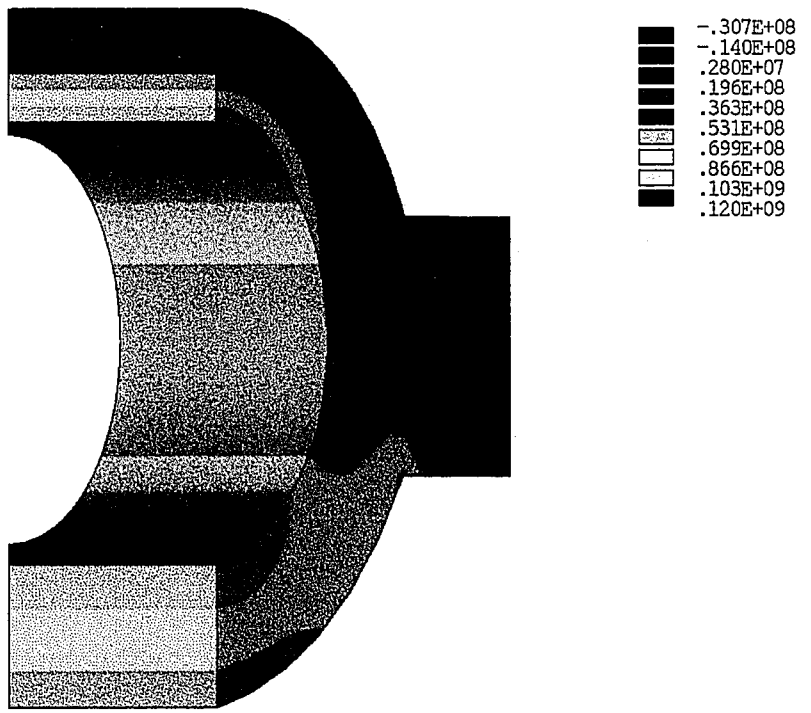

Figure 3.4: Steady state thermal stress from the 3-d view, σ_{zz}

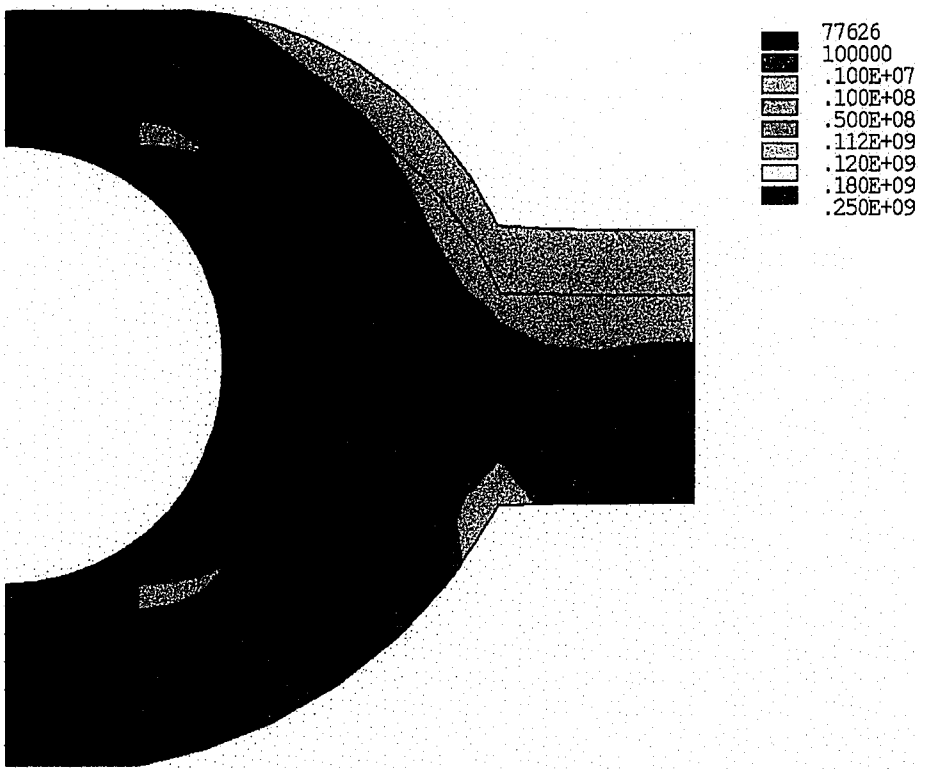

Figure 3.5: Transient thermal stress from the 3-d view at t=0 sec, σ_{zz}

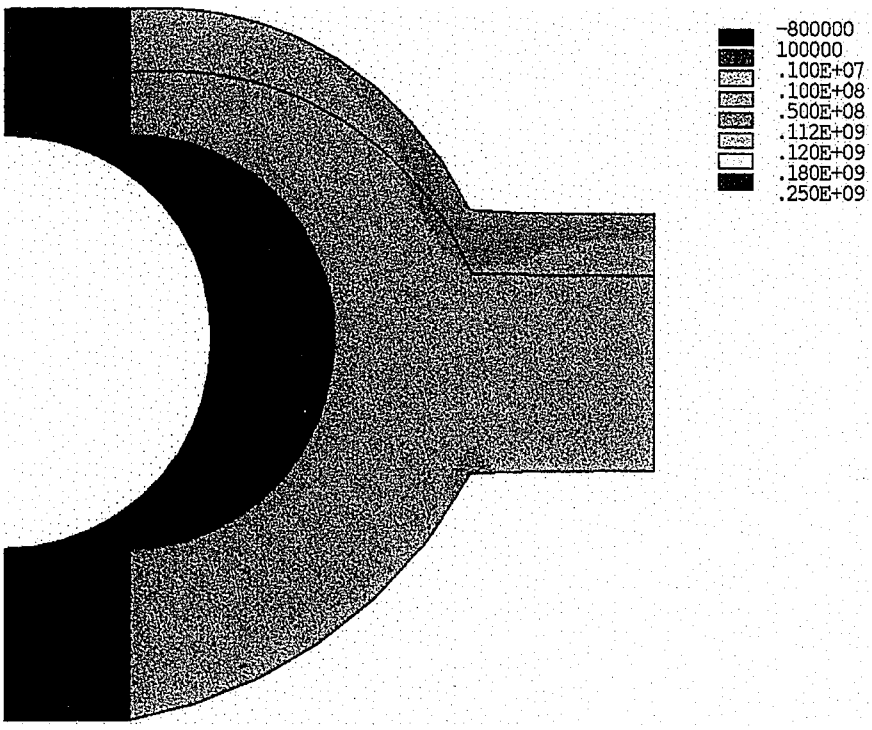

Figure 3.6: Transient thermal stress from the 3-d view at t=10 sec, σ_{zz}

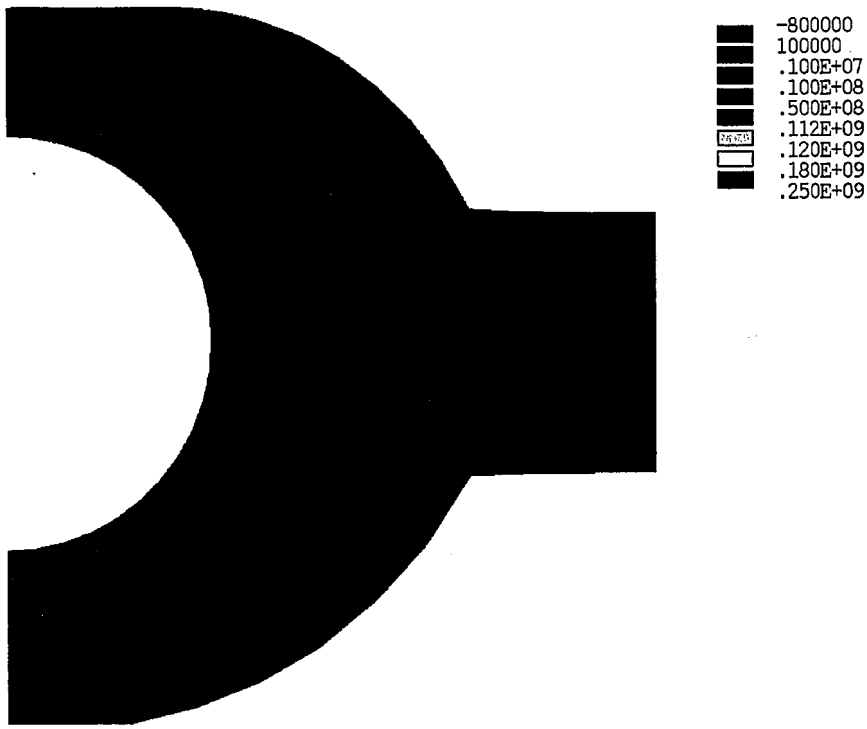

Figure 3.7: Transient thermal stress from the 3-d view at t=20 sec, σ_{zz}

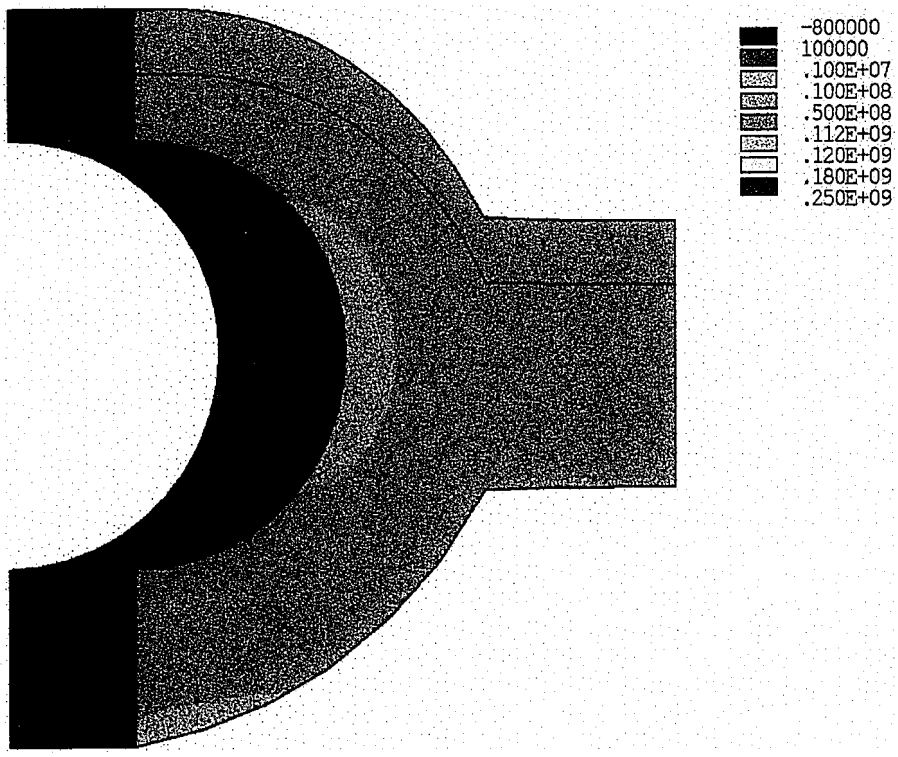

Figure 3.8: Transient thermal stress from the 3-d view at t=30 sec, σ_{zz}

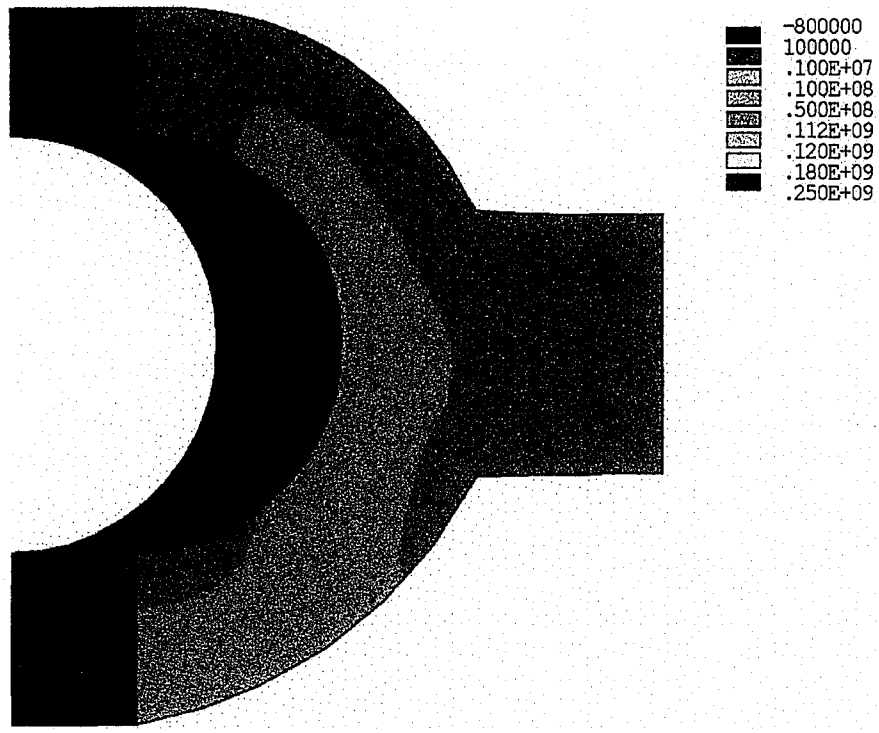

Figure 3.9: Transient thermal stress from the 3-d view at t=50 sec, σ_{zz}

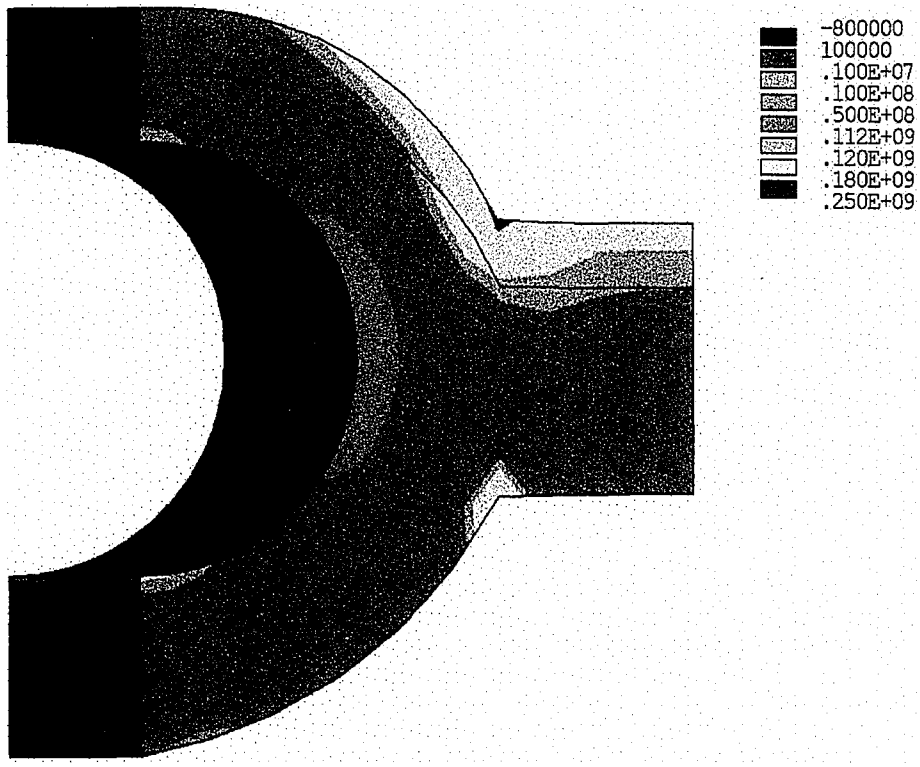

Figure 3.10: Transient thermal stress from the 3-d view at t=75 sec, σ_{zz}

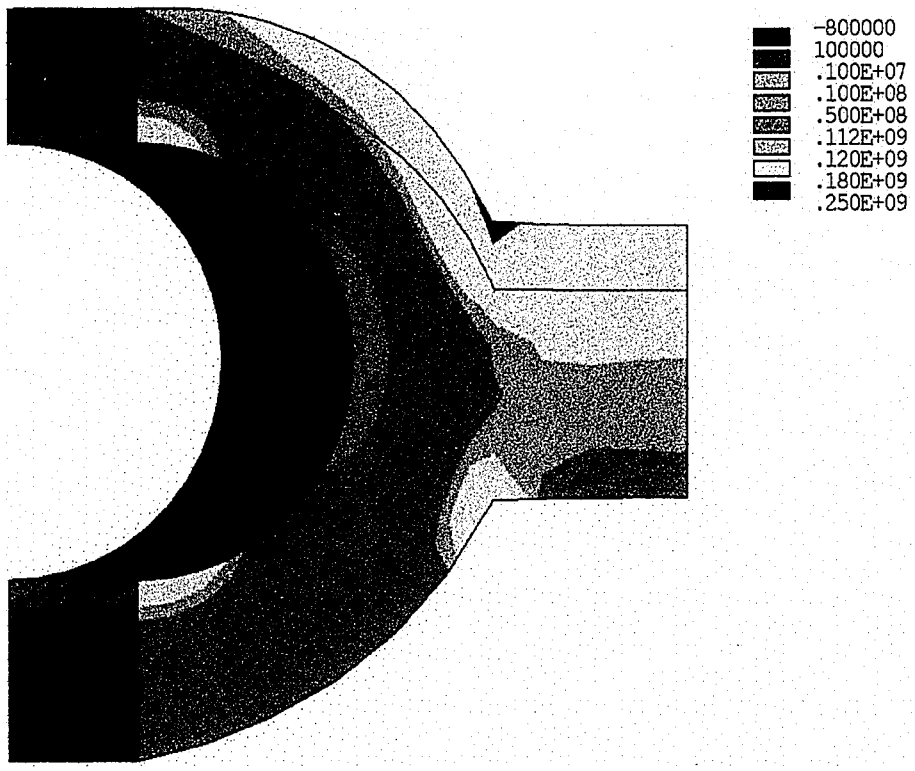

Figure 3.11: Transient thermal stress from the 3-d view at t=90 sec, σ_{zz}

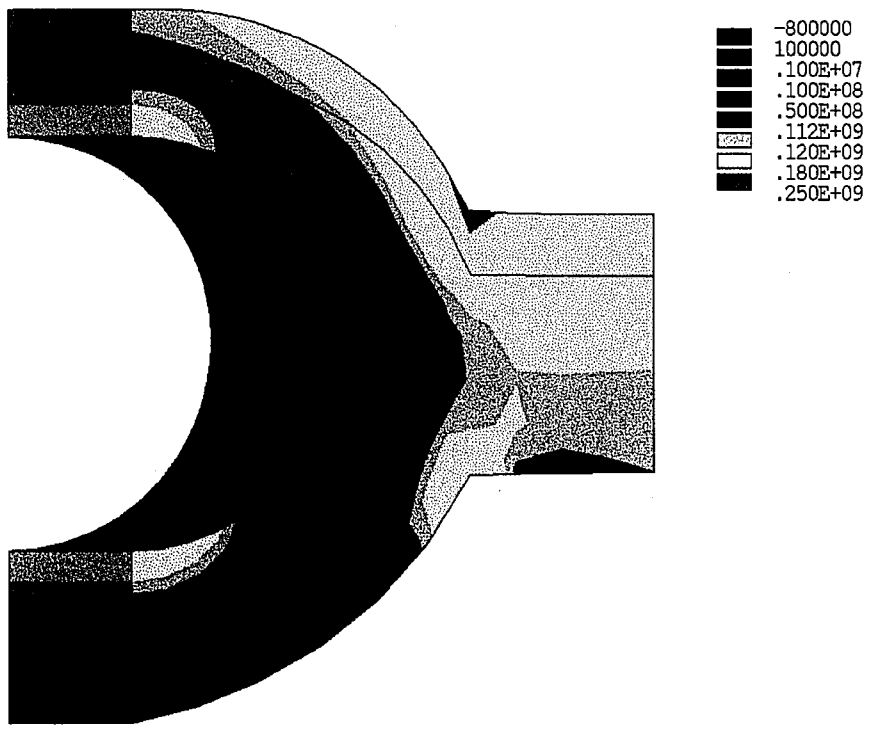

Figure 3.12: Transient thermal stress from the 3-d view at t=100 sec, σ_{zz}

4. Fracture Analysis

Three-dimensional fracture analysis for a semicircular surface crack was performed using enriched crack tip elements with FRAC3D, which was previously developed by Ayhan at Lehigh University. [13] This program uses an enriched finite element approach, which is very effective for obtaining stress intensity factors for general three-dimensional crack problems. In the enriched element approach, displacement compatibility is satisfied exactly on all element surfaces through the use of "transition" elements located between the enriched crack tip elements and the regular elements. These transition elements are simply enriched elements with an additional modifying factor that smoothly "zeros" the non-polynomial asymptotic behavior on surfaces shared with adjacent regular polynomial elements. For the finite element method to be used reliably in fracture mechanics, it is necessary to show that solutions converge numerically for a specific mesh and that successive mesh refinements result in improved accuracy. To satisfy these conditions, displacement compatibility must be maintained, while simultaneously increasing integration order and mesh refinement. 20 node quadratic hexahedron elements are used in FRAC3D calculations. In the absence of a crack, FRAC3D is capable of evaluating displacements and three dimensional stress states at the nodal points. When a crack or multiple cracks are present in the model, additionally, fracture parameters such as stress intensity factors and strain energy release rates are computed at the nodes along the crack front.

For the succeeding calculations, 24*24 integration order, which has the greatest impact on solution accuracy, was used to determine the stress intensity factors. Only K1

values were computed, K2 and K3 values were set zero as a constraint due to "mode 1" symmetric loading of the model.

The first stress intensity factor calculations performed were stress intensity factors due to residual stresses caused by welding. This can be determined by superposition by first computing σ_{zz}, which is equal to the yield strength of the overlay. –160 Mpa, σ_{zz}, was applied to the model (with crack) to calculate the stress intensity factors. The approach is shown in Figure 4.1. The computed stress intensity factors are shown in Figure 4.2 and the maximum stress intensity factor at $\Pi/2$ is shown in Figure 4.3 for different crack spacing values.

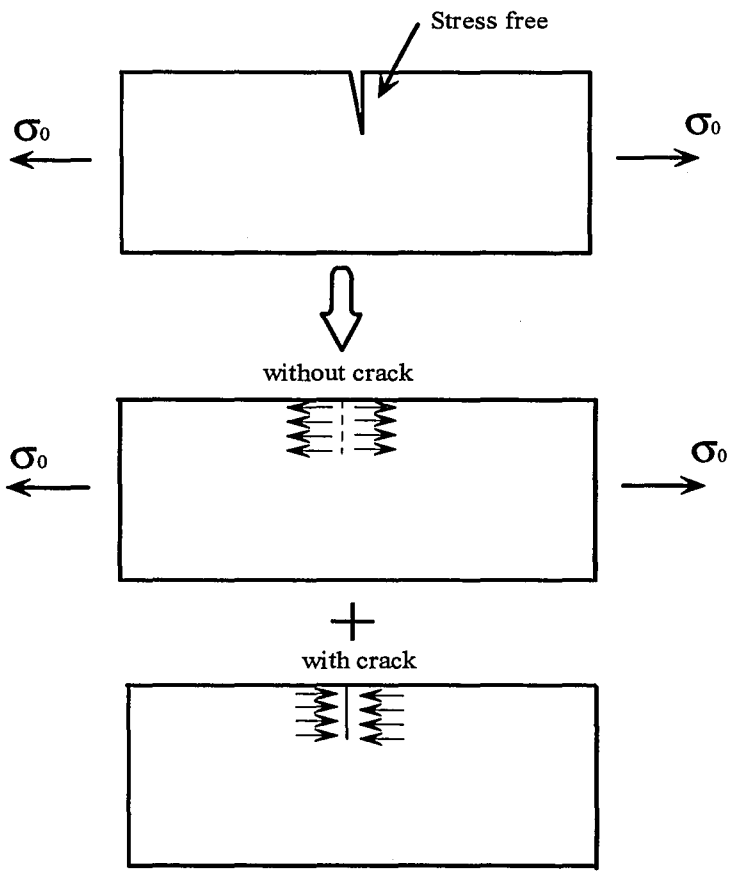

Figure 4.1: Superposition approach for computing K1 values due to residual stresses from welding

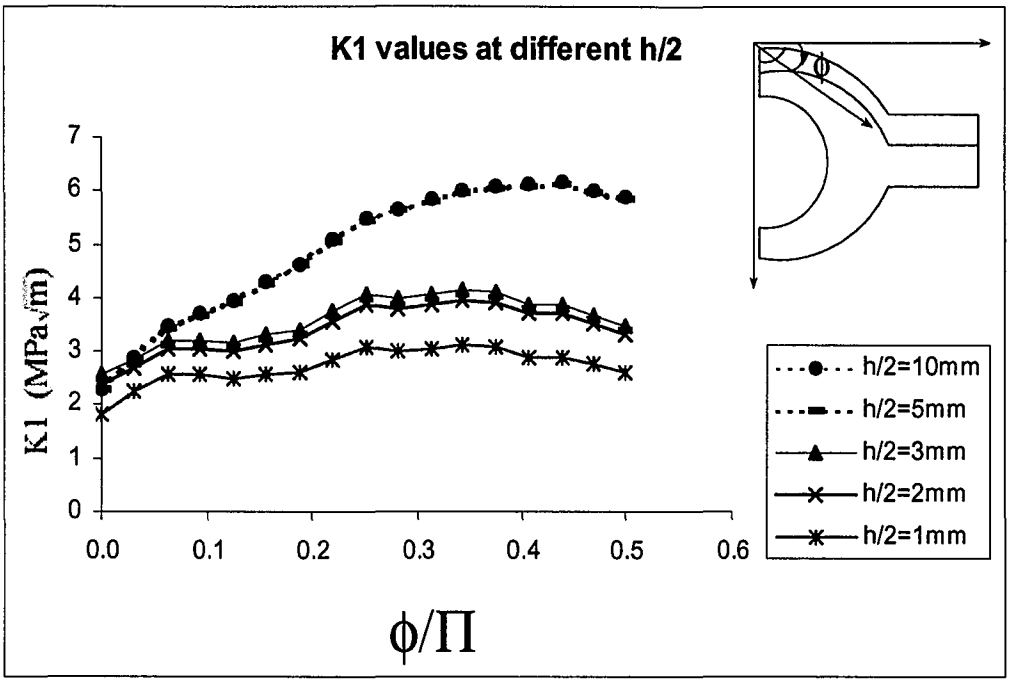

Figure 4.2: K1 values along the semicircular crack front due to residual stresses caused by welding

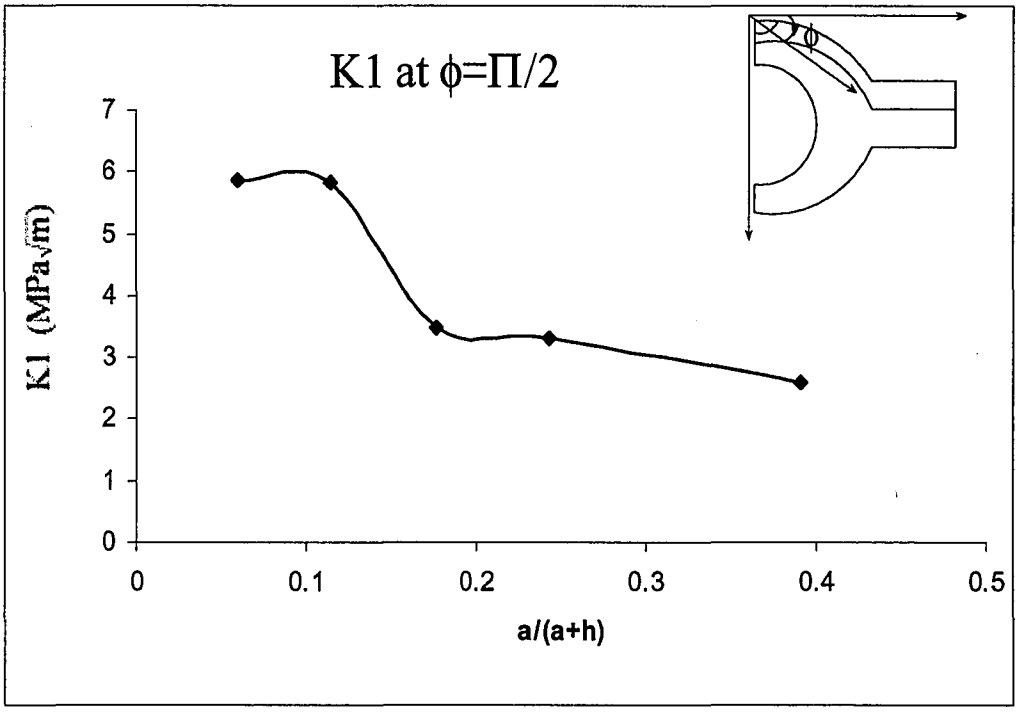

Figure 4.3: K1 values due to residual stresses caused by welding at the deepest point of crack penetration (a=crack depth, h=crack spacing)

The effect of tied nodes was examined by computing K1s in two different models. Everything is the same in the two models except for the boundary conditions on the z=h/2 plane. One model is fixed at h/2 (h is the crack spacing) and the other model is constrained by defining tied nodes at h/2. The stress intensity factors computed are shown in Table 4.1. As can be seen, there is very little difference between the resulting K1 values.

ϕ/Π	K1 ($MPa\sqrt{m}$)	K1 ($MPa\sqrt{m}$)
	fixed nodes	tied nodes
0	18.21	18.24
0.125	29.62	29.63
0.25	36.51	36.57
0.375	39.64	39.67
0.5	38.23	38.28

Table 4.1: Computed K1 values to examine the effect of "tied nodes" boundary condition

The stress intensity factors due to steady state thermal stresses computed next. Since, the fireside is in compression at steady state, the crack surfaces are closed. The values computed for steady state condition are very small negative values. Therefore, they can be accepted as zero for steady thermal conditions, K1 = 0.

For the final part of the problem, the stress intensity factors due to transient thermal stresses were computed. Transient thermal analysis was performed to obtain time dependent temperatures at the nodes from ANSYS. These time dependent temperatures at the nodes are input to FRAC3D and used to determine the stress intensity factors for the transient conditions. The computations were performed for five different h/2 (crack half-spacing) values, which are 1mm, 2mm, 3mm, 5mm and 10mm. The results are shown in Figures 4.4 to 4.8. The maximum stress intensity factors are obtained at the deepest point of penetration as shown in Figures 4.9 and 4.10. FRAC3D contour plots are shown in Figures 4.11 and 4.12 for h/2=3mm at t=100 sec. These plots show the axial stress, which is σ_{zz}. Since our reference temperature is 400 °C and the temperature at the fireside surface of the boiler tube reaches its minimum at t=100sec, maximum tensile stress values were obtained.

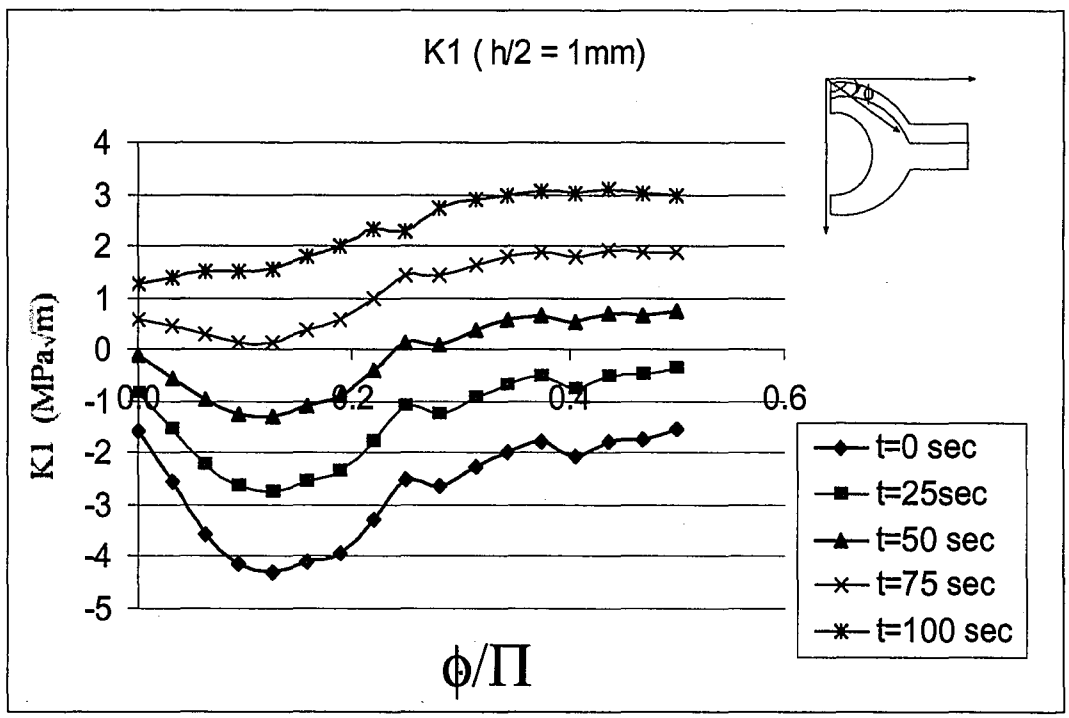

Figure 4.4: Transient stress intensity factors for crack spacing, h/2 = 1mm

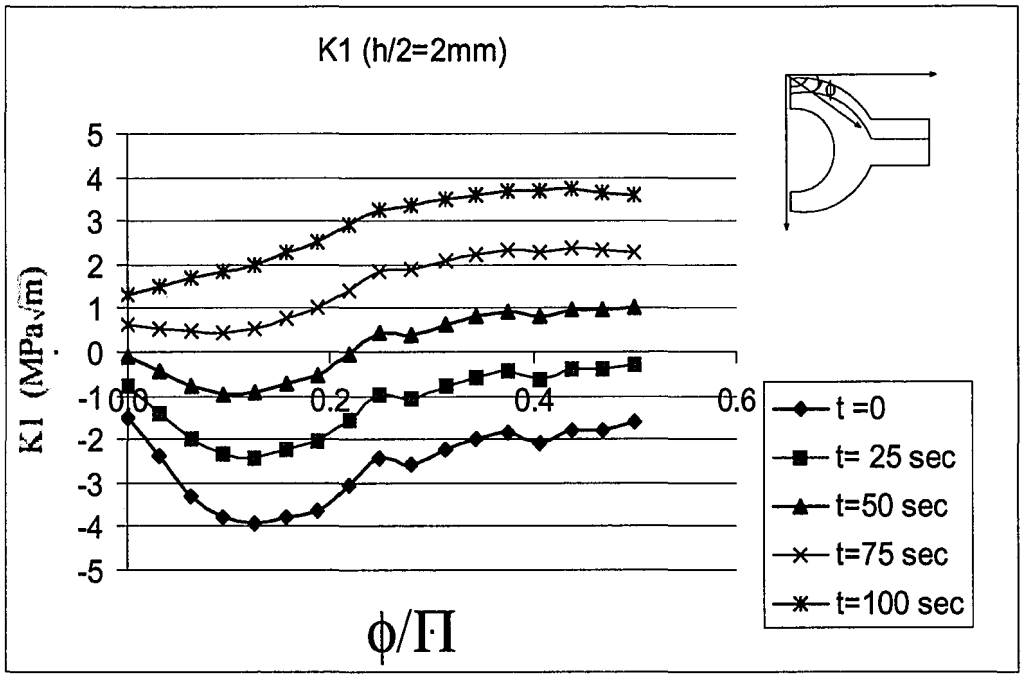

Figure 4.5: Transient stress intensity factors for crack spacing, h/2 = 2mm

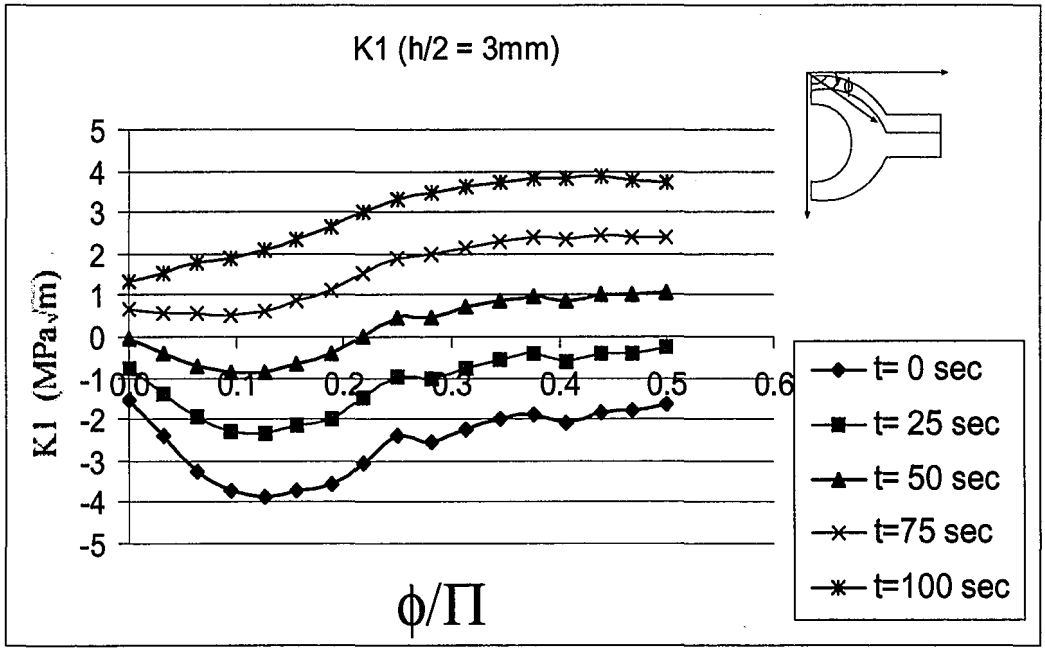

Figure 4.6: Transient stress intensity factors for crack spacing, h/2 = 3mm

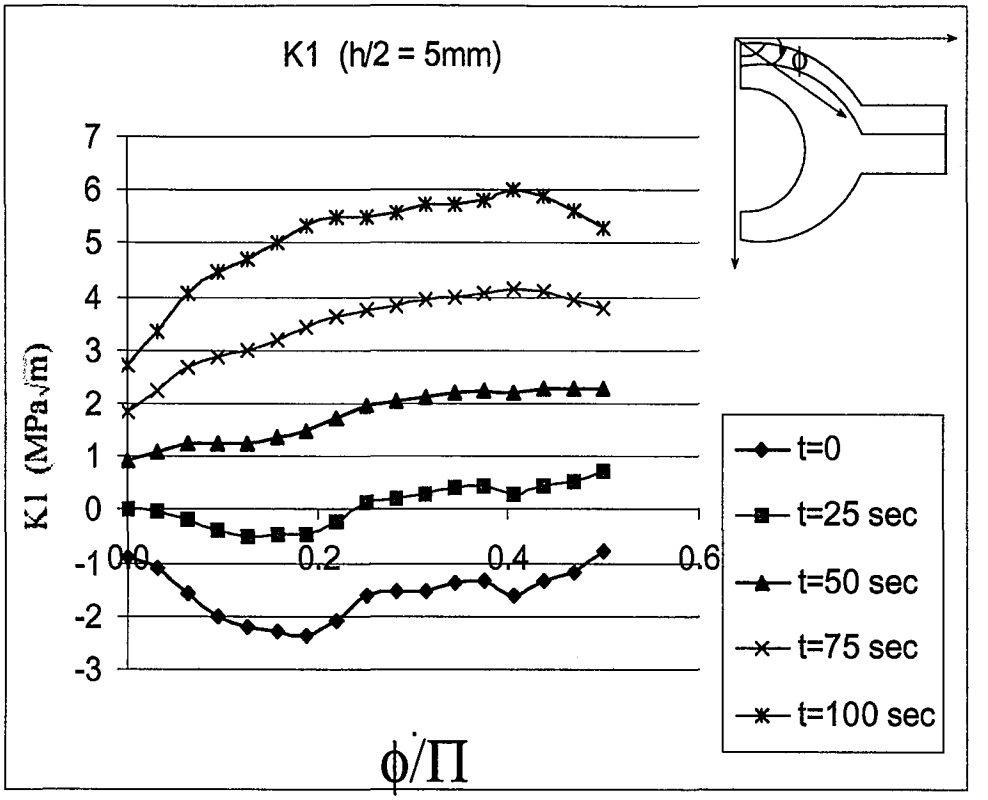

Figure 4.7: Transient stress intensity factors for crack spacing, h/2 = 5mm

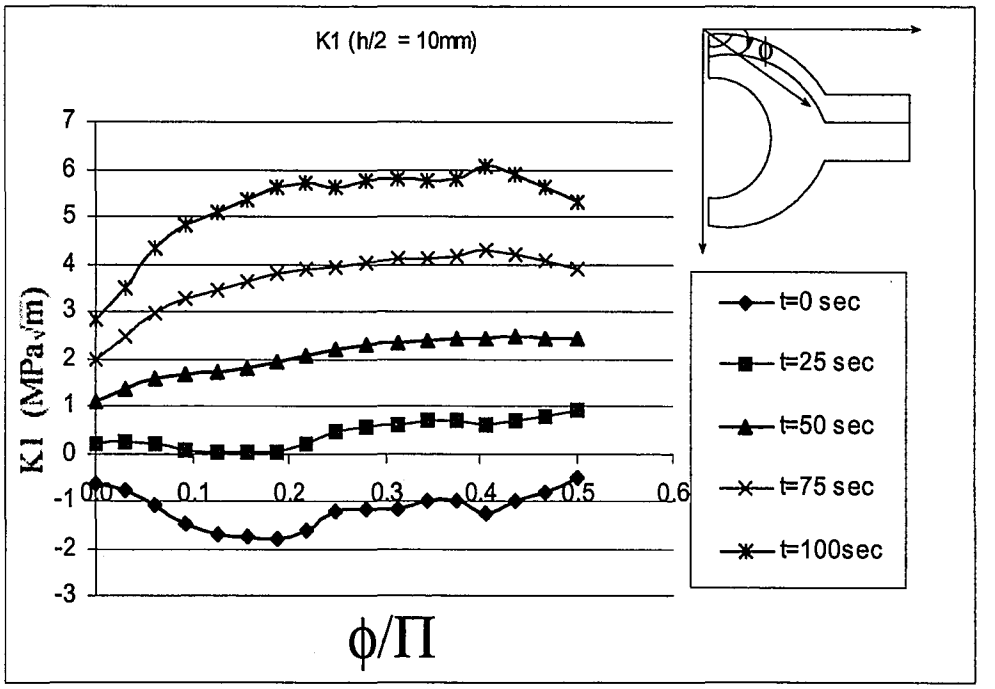

Figure 4.8: Transient stress intensity factors for crack spacing, h/2 = 10mm

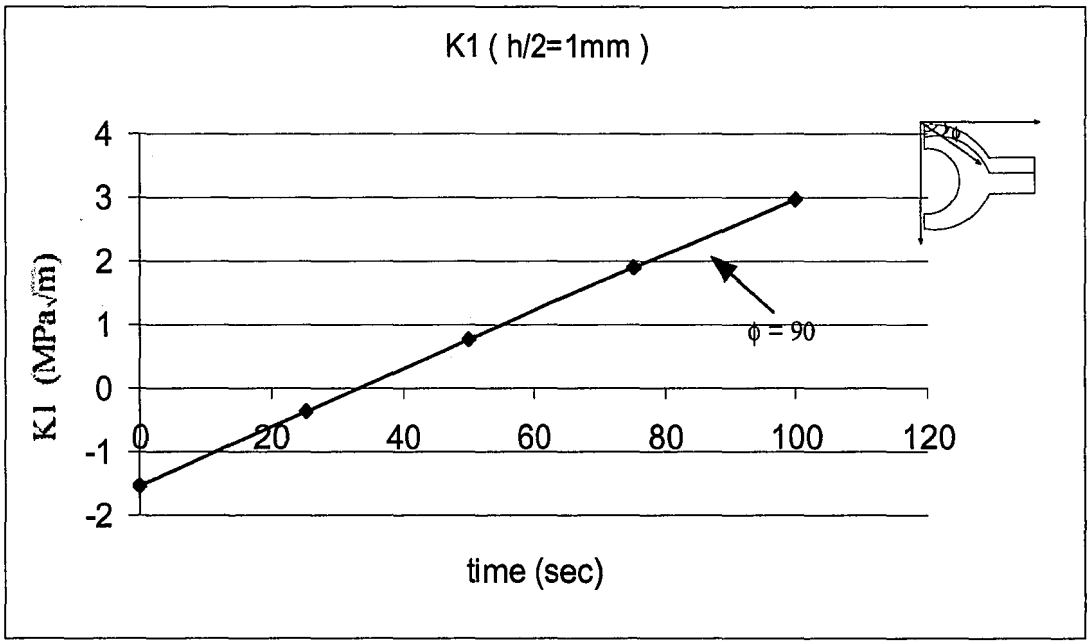

Figure 4.9: Transient stress intensity factors at ϕ equals to 90, for h/2 = 1mm

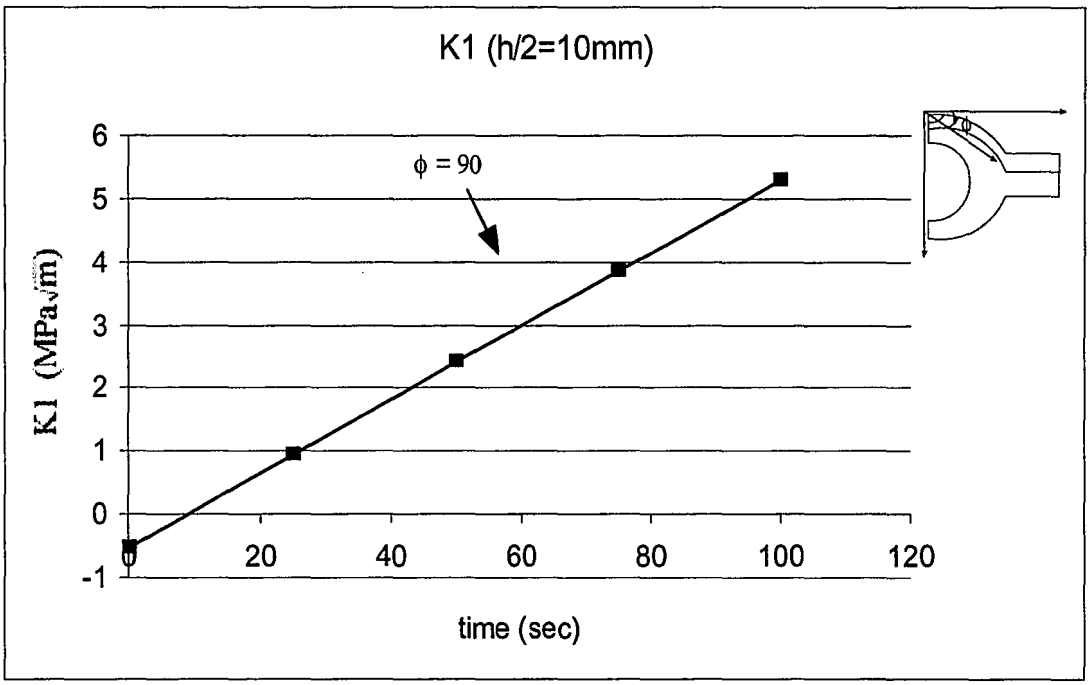

Figure 4.10: Transient stress intensity factors at ϕ equals to 90, for h/2 = 10mm

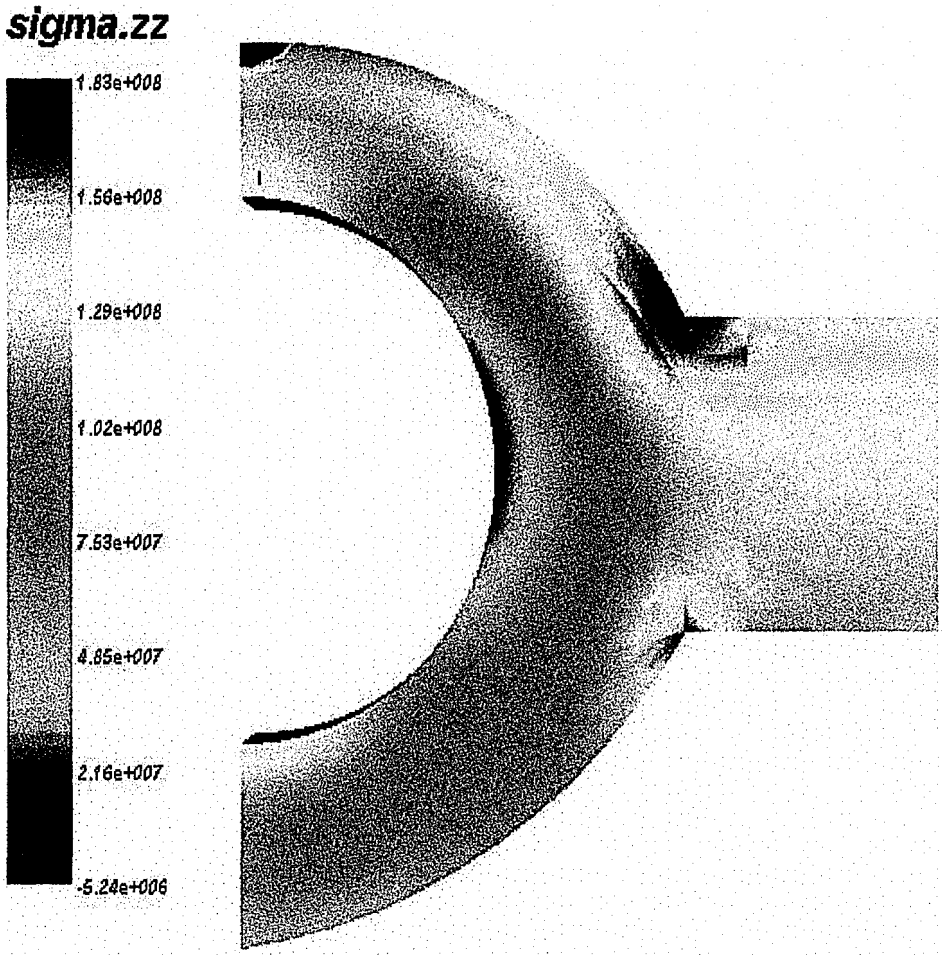

Figure 4.11: FRAC3D σ_{zz} contour plot of 3mm model at t=100 sec, front view

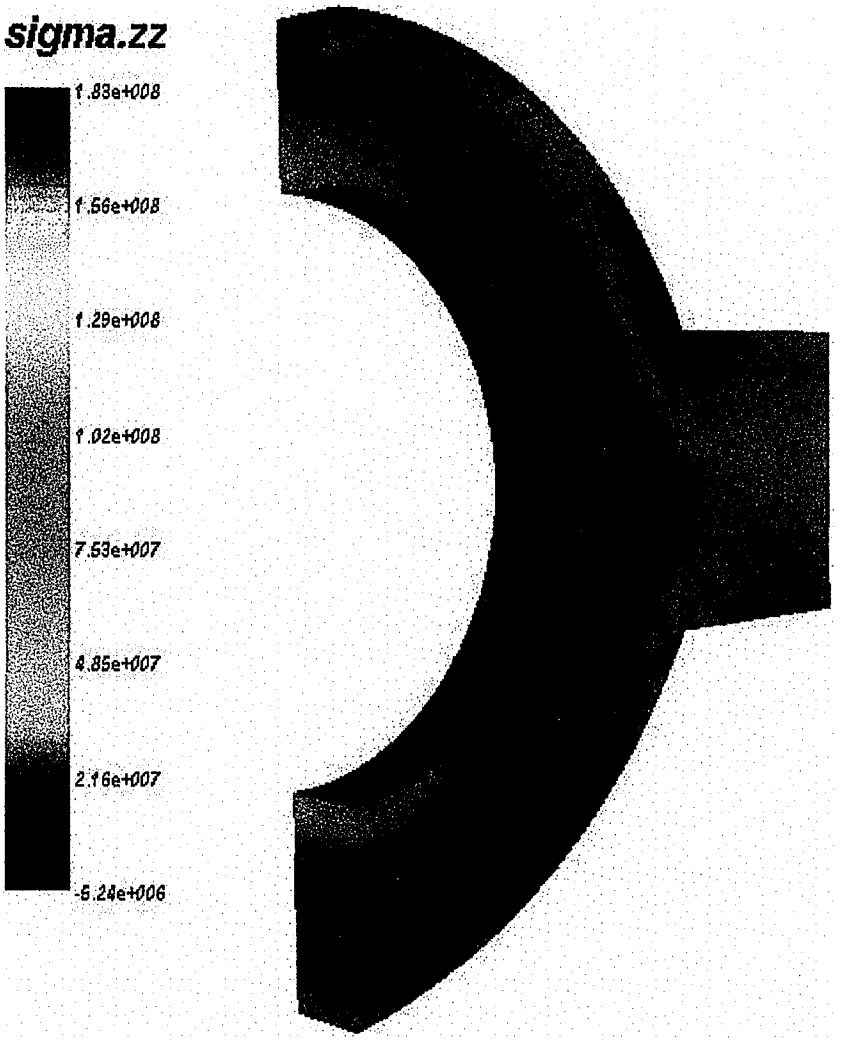

Figure 4.12: FRAC3D σ_{zz} contour plot of 3mm model at t=100 sec, 3-d view

We obtained ΔK, where $\Delta K=K_{max} - K_{min}$, approximately 6 $Mpa\sqrt{m}$ from the fracture analysis. The approximate fracture toughness value, K_{IC} of the overlay coating is around 120 $Mpa\sqrt{m}$. $K=K_{\Delta T}+K_{res}$, when K reaches K_{IC} failure occurs. Since we know the crack depth, the periodic crack spacing and the approximate K_{IC} value, the necessary ΔT to cause the cracking can be computed. The computed ΔT to cause cracking is very large, even more than 1000 °C. If the computed ΔT is very large then it is unlikely that the value for K_{IC} is the correct value to use. Corrosion effects must significantly lower K_{IC} for thermal cracking to be a plausible explanation for the cracking behavior.

5. Conclusions

Both 3-d and axisymmetric models were used to examine the mechanism of cracking in weld overlay boiler tubes. Transient thermal analyses were performed to obtain the temperature distributions due to soot blowing operations. All computations were performed using reference ΔT, which was 50 °C, in transient calculations.

Coupled structural analyses were performed to simulate the thermal stresses. High tensile thermal stress values those were close to two thirds of the yield strength, 100 MPa, were observed for 50 °C temperature difference due to cooling boundary conditions on the boiler tube fireside. Both temperature and stress results are shown as contour plots.

Stress intensity factors were generated for five different crack spacing for both welding residual stresses and transient thermal stresses. The maximum values are obtained at the deepest point of penetration for cracks with the greatest periodic spacing. As the crack spacing increases, the values of computed stress intensity factors also increase.

In conclusion, the first part, which was to determine ΔK, of remaining life assessment of circumferentially cracked weld overlay coatings is performed in this thesis. Tensile transient thermal stresses cause positive ΔK, which is the key parameter in fatigue life analysis.

References:

1. Chiew, S. P., Lie S.T., Lee C. K., Huang Z. W., "Stress Intensity Factors For a Surface Crack in a Tubular T-joint", Int. Journal of Pressure Vessels and Piping, 78(2001), pp. 677-685

2.Cao, J. J., Yang, G. J., Packer, J. A., Burdekin F. M., "Crack Modeling in FE Analysis of Circular Tubular Joints", Engineering Fracture Mechanics, 61(1998), pp. 537-553

3.Taylor, D., "Crack Modeling: A Technique for the Fatigue Design of Components", Engineering Failure Analysis, 3(1996), No. 2, pp. 129-136

4.Murugan, S., Kumar, P. V., Raj, B.,Bose, M. S. C., "Temperature Distribution During Multipass Welding of Plates", Int. Journal of Pressure Vessels and Piping, 75 (1998), pp. 891-905

5. Murugan, S., Rai, K.S.,Kumar, Jayakumar, T., Raj, B.,Bose, M. S. C., "Temperature Distribution and Residual Stresses due to Multipass Welding in type 304 Stainless Steel and Low Carbon Steel Weld Pads", Int. Journal of Pressure Vessels and Piping, 78 (2001), pp. 307-317

6. Webster, G. A., Ezeilo, A. N., "Residual Stress Distributions and Their Influence on Fatigue Lifetimes", Int. Journal of Fatigue, 23 (2001), pp. 375-383

7. Sarkani, S., Tritchkov, V., Michaelov, G., "An Efficient Approach For Computing Residual Stresses in Welded Joints"

8.Fricke,S., Keim, E., Schmidt, J.,"Numerical Weld Modeling – A Method for Calculating Weld-induced Residual Stresses ", Nuclear Eng. and Design, 206(2001), pp.139-150

9. Kou, Sindo, Welding Metallurgy, New Jersey: Wiley, 2002

10. ANSYS, Inc.-Thermal Analysis Guide, Ansys Relese 5.6, November 1999

11. Yildirim,B., Nonlinear Thermal Stress/Fracture Analysis of Multilayer Structures using Enriched Finite Elements, Bethlehem, Lehigh University, PhD Thesis,2000

12. Erskine, C. P., Effect of The Coefficient of Thermal Expansion of a Coating on Waterwalls in a Super-Critical Coal Fired Utility Boiler, Bethlehem, Lehigh University, M. S. Thesis, 1991

13. Ayhan, A. O., Nied, H. F., "Stress Intensity Factors for Three-Dimensional Surface Cracks Using Enriched Finite Elements", Int. Journal for Numerical Methods in Engineering, 54(2002), pp. 899-921

14. http://www.robot-welding.com/arc_welding_parameters.htm

15. Luer, K., DuPont, J. N., Marder, A. R., Skelonis, C., "Corrosion fatigue of alloy 625 weld claddings in combustion environments", Materials at High Temperatures, 18(2001), pp. 11-19

Appendix ANSYS Procedure

This is the ANSYS procedure used in this study. This parametric input file performs the transient thermal analysis first. Then, it inputs the obtained temperatures to the structural analysis to compute the transient thermal stresses.

```
/PREP7
/TITLE, BOILER_TUBE
ANTYPE,4,NEW
ET,1,PLANE77     &ET,2,SOLID90
MAT,1    &REAL,1    &TYPE,1
!MAT PROPERTIES FOR SA213/T12
MP,KXX,1,38       !CONDUCTIVITY W/M.C
MP,DENS,1,7829    !DENSITY KG/M3
MP,C,1,402.6,0.632  !SPECIFIC HEAT  J/KG.C
!MAT PROPERTIES FOR 309S
MP,KXX,2,18.7       !CONDUCTIVITY W/M.C
MP,DENS,2,8030      !DENSITY KG/M3
MP,C,2,502          !SPECIFIC HEAT  J/KG.C
C**** MEASURED TUBE DIMENSIONS
WL=0.00889          !WEB LENGTH(M)
THC=0.00254         !COATING THICKNESS(M)
THW=0.00533         !WEB THICKNESS(M)
```

```
RI=0.009017          !INNER RADIUS(M)

THB=0.006787         !BOILER BOTTOM THICKNESS

LCW=0.015672 !CENTER TO WEB LENGTH

T1=THB+RI-THW

!KEYPOINTS

K,1,0,0  K,2,,THB  K,3,,T1+THW  K,4,LCW,T1  K,5,LCW,T1+THW+THC

K,6,LCW+WL,T1  K,7,LCW+WL,T1+THW+THC  K,8,LCW+WL,T1+THW+2*THC

K,9,LCW,T1+THW+2*THC  K,10,,THB+2*RI+2*THC  K,11,,THB+2*RI+THC

K,12,,THB+2*RI  K,13,RI,THB+RI  K,14,LCW/2,T1/2-THC

K,15,0.4*LCW,THB+2*RI+2*THC/3  K,16,0.4*LCW,THB+2*RI+5*THC/3


LARC,11,5,15  LARC,10,9,16  LARC,1,4,14  LARC,12,2,13,RI

L,15,16  L,10,11  L,11,12  L,1,2  L,4,5  L,4,6  L,6,7

L,7,5  L,7,8  L,8,9  L,9,5


LGLUE,1,2,5


LDIV,18,,,4  LDIV,6,,,4


K,23,0.0011,0.0295  K,24,0.00238,0.0288  K,25,0.0038,0.0282


BSPLIN,20,23,17  BSPLIN,21,24,18  BSPLIN,22,25,19
```

LESIZE,3,,,6 LESIZE,9,,,4 LESIZE,10,,,4 LESIZE,11,,,4 LESIZE,12,,,4

LESIZE,14,,,4 LESIZE,13,,,2 LESIZE,15,,,2 LESIZE,16,,,6 LESIZE,17,,,6

LESIZE,8,,,6 LESIZE,5,,,2

LESIZE,20,,,4 LESIZE,2,,,4 LESIZE,1,,,4 LESIZE,18,,,8

LESIZE,26,,,8 LESIZE,25,,,8 LESIZE,24,,,8 LESIZE,6,,,8 LESIZE,21,,,4

LESIZE,22,,,4 LESIZE,23,,,4 LESIZE,7,,,6 LESIZE,19,,,6

AL,6,24,18 AL,21,25,1,24 AL,22,26,2,25 AL,23,19,5,20,26 AL,5,16,15,17

AL,15,12,13,14 AL,9,10,11,12 AL,8,3,9,16,19,7,4

LCCAT,5,19

ASEL,S,AREA,,1,7 AMESH,ALL

ASEL,INVE AMAP,8,1,2,11,12 ASEL,ALL

LSEL,S,LCCA LDEL,ALL LSEL,ALL

ESIZE,,3 VEXT,1,8,,,,0.001

ESIZE,,7 VEXT,1,8,,,,-0.009

ACLEAR,ALL

```
!ASSIGN ATTRIBUTES OF ELEMENTS
VSEL,S,VOLU,,1,6  VSEL,A,VOLU,,9,14
ALLSEL,BELOW,VOLU   MPCHG,2,ALL   ALLSEL,ALL

ASEL,S,,,12   ASEL,A,,,16   ASEL,A,,,20
ASEL,A,,,25   ASEL,A,,,27   ASEL,A,,,33
ASEL,A,,,46   ASEL,A,,,50   ASEL,A,,,54
ASEL,A,,,59   ASEL,A,,,61   ASEL,A,,,67
CM,FIRE,AREA

ASEL,ALL
ASEL,S,,,37   ASEL,A,,,76   ASEL,A,,,71   ASEL,A,,,42
CM,AIR,AREA

ASEL,ALL   ASEL,S,,,74   ASEL,A,,,40
CM,WATER,AREA   ALLSEL,ALL
FINISH

/SOLU
TIMINT,OFF,THERM   DA,FIRE,TEMP,400
SFA,AIR,,CONV,5,200   DA,WATER,TEMP,370
KBC,1   TIME,1E-6
LSWRITE,1   TIMINT,ON,THERM
```

DDELE,FIRE,TEMP DA,FIRE,TEMP,350 TIME,100

DELTIM,0.8,0.01,1 KBC,0 LSWRITE,2

OUTRES,ALL,ALL LSSOLVE,1,2 FINISH

/PREP7

ET,2,SOLID95

MP,EX,1,180E9 MP,ALPX,1,1.4E- MP,NUXY,1,0.3

MP,EX,2,140E9 MP,ALPX,2,1.76E-5 MP,NUXY,2,0.27

NSEL,S,LOC,Z,-0.009 NSEL,A,LOC,Z,0.001 D,ALL,UZ,0

NSEL,ALL NSEL,S,LOC,X,0.024562 NSEL,R,LOC,Y,0.016377

D,ALL,UY,0

NSEL,ALL NSEL,S,LOC,X,0 NSEL,A,LOC,X,0.024562

D,ALL,UX,0 ALLSEL,ALL

FINISH

/SOLU

TREF,400

LDREAD,TEMP,2,,,,,rth

SOLVE

FINISH

Vita

The author was born to Hasibe and Saim CITIRIK on July 3, 1979 in Adana, Turkey. He completed his primary and secondary school in Adana in June 1994. He went to Gazientep Fen Lisesi and graduated in 1997. The following year he started at Bosphorus University. He got his Bachelor of Science from Bosphorus University in Civil Engineering in 2001.

He came to the United States in August 2001. He started his graduate study at Lehigh University in Mechanical Engineering and Mechanics. He expects to get his Master's degree in May 2003.

END OF TITLE